

**IMMUNOASSAY-BASED MICROSENSING**

by

**Maurice Elie Jabbour**

---

Copyright © Maurice Elie Jabbour 2005

A Thesis Submitted to the Faculty of the

**BIOMEDICAL ENGINEERING PROGRAM**

In Partial Fulfillment of the Requirements  
For the Degree of

**MASTER OF SCIENCE  
WITH A MAJOR IN BIOMEDICAL ENGINEERING**

In the Graduate College

**THE UNIVERSITY OF ARIZONA**

**2005**

### STATEMENT BY AUTHOR

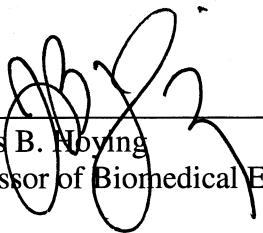
This thesis has been submitted in partial fulfillment of requirements for an advanced degree at The University of Arizona and is deposited in the University Library to be made available to borrowers under rules of the Library.

Brief quotations from this thesis are allowable without special permission, provided that accurate acknowledgment of source is made. Requests for permission for extended quotation from or reproduction of this manuscript in whole or in part may be granted by the copyright holder.

SIGNED:  Aug - 5 - 2005

### APPROVAL BY THESIS DIRECTOR

This thesis has been approved on the date shown below:

 August 4, 2005  
James B. Noying Date  
Professor of Biomedical Engineering

## ACKNOWLEDGMENTS

I am thankful to the advice and guidance of my advisor, James B. Hoying, throughout this project. I am grateful for his mentoring support, which has helped me in advancing my graduate career. I am also indebted to the advice and help from the rest of my committee members: Pierre Deymier, Roberto Guzman, Hugh Barnaby, and Joel Cuello.

Due to the interdisciplinary nature of this project, I offer my thanks to all the people who helped me during the past two years. Specifically, I want to thank Sarah Dahl and Sean Essex for their help around the microelectronic laboratory; Thanks to Prof. Jeanne Pemberton, Dr. Paul Lee, Piotr Macech, and Valeria Ochoaval (Department of Chemistry) for their assistance with surface chemistry analysis; Thanks to Mike Morrell (Optical Sciences Center) and Ray Kraatz (Agilent Tech, Tempe AZ) for kindly providing a digital oscilloscope for my sensor analysis. I would like to thank the support of all members of the laboratory of Prof's J. Hoying, S. Williams and H. Barnaby, especially Helen Chen, Shaleen Beck, Mark Schwartz, Faith Rice, Alice Stone, Adam Hoying, and Jie Chen for their laboratory assistance.

In addition, I am grateful for the financial support provided by the NSF NIRT in Nanoelectronics (grant # 0303863) and the College of Engineering, University of Arizona.

Foremost, I appreciate the support of my family especially the support of Prof. Ghassan Jabbour.

## TABLE OF CONTENTS

LIST OF ILLUSTRATIONS.....	5
LIST OF TABLES.....	8
ABSTRACT.....	9
CHAPTER 1 REVIEW OF IMMUNOASSAY-BASED BIOSENSORS.....	11
1.1 INTRODUCTION .....	11
1.2 OVERVIEW OF BIOSENSORS.....	12
1.3 PROTEIN IMMOBILIZATION.....	17
1.3.1 SURFACE CHEMISTRY EFFECT ON PROTEIN ADSORPTION .....	18
1.3.2 IMMOBILIZATION METHODS FOR IMMUNOASSAY .....	21
1.4 PROTEIN PATTERNING FOR IMMUNOASSAY .....	23
1.4.1 MICROARRAY PATTERNING FOR IMMUNOASSAY .....	27
1.5 IMMUNOASSAY-BASED BIOSENSOR.....	29
1.5.1 EXAMPLES OF COMMERCIAL BIOSENSORS.....	32
1.6 SUMMARY AND PROPOSED BIOSENSOR DESIGN.....	34
CHAPTER 2 ANTIBODY ATTACHMENT TO FUNCTIONALIZED SILICA	
SUBSTRATES .....	36
2.1 INTRODUCTION .....	36
2.2 SUBSTRATE MODIFICATION .....	37
2.3 GPTS COATING CHARACTERIZATION .....	39
2.4 IMMUNOASSAY MEASUREMENTS.....	46
2.4.1 EXPERIMENTAL PROCEDURE.....	46



2.4.2 RESULTS AND DISCUSSION .....	48
2.5 SUMMARY AND CONCLUSION .....	54
CHAPTER 3 TOWARD AN IMMUNOASSAY-BASED BIOSENSOR .....	56
3.1 INTRODUCTION .....	56
3.2 BACKGROUND ON AVALANCHE PHOTODIODES .....	56
3.3 EXAMPLES OF APD APPLICATIONS .....	59
3.4 CHARACTERIZATION OF PHOTODIODES .....	60
3.5 APD DETECTION OF CHEMILUMINESCENCE .....	63
3.5.1 EXPERIMENTAL PROCEDURE .....	63
3.5.2 RESULTS AND DISCUSSION .....	66
3.6 SUMMARY AND CONCLUSION .....	72
CHAPTER 4 SUMMARY AND FUTURE WORK .....	73
4.1 SUMMARY .....	73
4.2 FUTURE WORK .....	74
APPENDIX A .....	77
REFERENCES .....	78

## LIST OF ILLUSTRATIONS

Figure 1.1 – Components of a typical biosensor. As depicted, specificity is a key property for a biosensor. (Redrawn from M. Keusgen [4]) .....	12
Figure 1.2 – Structure of an IgG. Shown are the variable and constant domains. Variable chains ( $V_H$ and $V_L$ ) form the antigen binding site. ....	14
Figure 1.3 – Immunoassay techniques. A generic immunoassay is shown in panel (a) while a sandwiched immunoassay is depicted in panel (b). Antibody as well as antigen can be tagged with fluorescent molecules .....	16

Figure 1.4 – Chemical structures of common silane compounds. ....	18
Figure 1.5 - Effect of surface chemistry on antibody orientation. (Redrawn from Chen <i>et al.</i> ) .....	20
Figure 1.6 – Microcontact printing (a), microfluidic network (b), and electrospray deposition (c) are shown. For detailed description, refer to text. (Redrawn from refs. [32, 34, 35]). Several steps are needed to form a protein microarray using microcontact printing as shown in panel (a). In panel (b), the immobilization of antibodies using microfluidic methods requires the flow of antibody solution and removal of microfluidic channels thereafter. Antibody-patterned substrate is incubated in fluorescently labeled antibodies. Fluorescent microscopy is used to image the substrate. Electron spray deposition technique is shown in panel (c). ....	25
Figure 1.7 – Principle of SPR detection. As the light source strikes the metal surface of the glass substrate, surface plasmon wave is emanated from the gold material. Difference in the angles of reflection is related to the formation of antibody-antigen complexes in solution. ....	33
Figure 2.1 – Proposed design for a portable, on-chip readout immunoassay-based sensor. ....	37
Figure 2.2 – A scheme for antibody attachment on GPTS coated silicon substrate. The silanization process occurs via a three-step mechanism as explained in the text. Regarding antibody attachment, any amine group on the antibody could react with the epoxy group on the substrate, although the location of NH <sub>2</sub> on the antibody as shown here is more desirable for our immunoassay. ....	38
Figure 2.3 – Flow chart for FTIR measurements and analysis. ....	41
Figure 2.4 – FTIR spectra for silica grown on gold and neat GPTS on KBr pellets. The silica presence on Au layer is indicated by the strong SiOSi vibration. For GPTS, the absence of SiOCH <sub>3</sub> shown around 820 on silicon will indicate the presence of the coating. ....	41
Figure 2.5 – FTIR data on GPTS coated substrates. Time and concentration variations are illustrated. Spectra shown for each solution condition are the average of three replicates. ....	43
Figure 2.6 – AFM images of bare SiO <sub>2</sub> and GPTS-coated silicon oxide layer. The roughness of SiO <sub>2</sub> and GPTS coating were 0.120 nm, and 0.245 nm, respectively. ....	45
Figure 2.7 –Immunoassay protocol used in antibody attachment and detection. A radiography image of one experiment is depicted in the center of this scheme. ....	47

- Figure 2.8 - Generation of chemiluminescence through reaction between an organic substrate (luminol) with peroxidase. In this case, visible but dim blue light is emitted. (\* indicates an excited state emitter). ..... 48
- Figure 2.9 – Data on primary antibody attachment to the GPTS-coated silicon oxide layer..... 49
- Figure 2.10 – Dosage experiment. Four dilution factors were used in the preparation of 1° Ab solutions. The template shown in panel (a) was followed during the spotting of antibodies solutions. The results of the dosage experiment are shown in panel (b). 51
- Figure 2.11 – Mouse monoclonal anti-biotin IgG printed on GPTS-coated silicon dioxide in 1:100, 1:500, 1:1000, and 1:5000 dilution factors in the pattern shown in panel (a). Panels (b) and (c) depict radiography images of the assay to detect biotin conjugated to HRP. .... 53
- Figure 2.12 – A 1:100 Mouse anti-biotin IgG was printed in a 6x5 array on two 1 in<sup>2</sup> GPTS coated silicon oxide layers. One sample was immersed in a biotin\_HRP solution while another sample was immersed in a buffer solution as shown panels (a) and (b). As expected no signal was observed for panel (b). .... 54
- Figure 3.1 – Principle of detection of a typical APD is depicted in panel (a). Panel (b) illustrates a more complex design of an APD developed by C. Jackson for single photon detection (redrawn from S. Kasap and C. Jackson *et.al.* [50, 51]). .... 57
- Figure 3.2 – Current vs. Voltage (IV) curve of an avalanche photodetector. The Geiger-mode is the region where APD can detect single photon. (Reprinted from C. Jackson with permission[49]) ..... 58
- Figure 3.3 – As shown in the design layout of an APD array, the size of the array is slightly above 1mm<sup>2</sup>. Panel (b) shows a top-down view of a packaged APD. A magnified view of the dotted square is depicted in panel (c). .... 60
- Figure 3.4 – Diode Characteristic (a) and Breakdown voltage (b). .... 61
- Figure 3.5 – APDs characterization using a red light emitting diode (LED). Shown in panels (a) and (b) are the circuits used to test the detection of light using APDs. The voltage across the red LED was varied from 0V to 4V changing the intensity of light. The voltage was measured across the resistor of the APD being tested using an oscilloscope. Panels (c) and (d) show the voltage readout indicating the capability of APDs to detect light emanating from the red LED. .... 62

Figure 3.6 – Oscilloscope output. Voltage is labeled as y-axis (note 5V per division). Voltage values shown in panels (a) and (b) are taken at two different time intervals. The decrease in voltage is due to the decay of chemiluminescence over time..... 65

Figure 3.7 – Reusability of APD packages after a piranha cleaning procedure. The number in parentheses on the x-axis indicates the number of piranha cleaning performed. The cleaning allowed us to use the two APD packages to perform eight experiments..... 67

Figure 3.8 – APD detection of chemiluminescence. ‘Experiment’ refers to 1<sup>o</sup> Ab attached to APD whereas ‘control’ refers to PBS being printed on APDs. Clearly, APDs are sensing the secondary Ab recognition of the primary Ab as indicated by the difference in voltages between ‘experiments’ ( $\Delta$ ,  $\square$ , and  $\circ$ ) and ‘controls’ ( $\blacktriangle$ ,  $\blacksquare$ , and  $\bullet$ )..... 68

Figure 3.10 – APD detection of chemiluminescence using an immunoassay based on anti-biotin IgG-biotin conjugated to HRP interactions. Experimental schemes used are shown. .... 70

Figure 3.11 – APD detection of chemiluminescence after background subtraction. The curve is more descriptive of the chemiluminescence decay in the presence of HRP. .... 72

Figure 4.1 - Improving the optics of the developed immunoassay-based microdevice.... 76

## LIST OF TABLES

Table 1 – Experimental conditions for FTIR experiment..... 40

## ABSTRACT

Immunoassay systems are recognized as superior modalities for detecting biological substances. Immunoassay sensing offers the advantages of selectivity and sensitivity. Development of a portable micro-immunoassay system is quite desirable for fieldwork applications. The basis of such portable sensing approach would combine molecular printing techniques with solid-state devices. In this work, I report on advances in attaching and patterning antibodies on  $\text{SiO}_2$  substrates with the aim of retaining their biological functionality. The integration of functional antibodies with conventional photodetectors through direct printing onto the oxide layer of the detector will result in a device with on-chip readout. To that effect, monoclonal IgG antibody was printed onto chemically modified and thermally oxidized silicon substrates. Using a generic immunoassay, I was able to validate the activity of the antibody adsorbed on epoxy-terminated silane surface coatings. An assay based on Mouse anti-biotin – Biotin conjugated to horseradish peroxidase interaction was used to show the activity of printed antibody, specifically the molecular orientation of the antibody, on the silane-coated surface. In addition, avalanche photodiodes were used as solid-state detector for light detection. Avalanche photodiodes were able to detect the chemiluminescence, an indication of the sensitivity of the sensor for the immunoassay. Furthermore, there were clear differences between 'control' measurements obtained using a saline buffer solution compared to actual measurements obtained from antibody attachment to the surface of the sensor. This difference in signals is an indication that protein-protein interaction

occurred. To that effect, on-chip readout, namely in situ measurement of light detection without the aid of additional detector, was shown.

In summary, I present, as a proof of concept, one example of immunoassay-based microsensensing through the integration of antibody with avalanche photodiodes. This may have potential application in designing commercial, low cost, and portable biosensors.

## **CHAPTER 1**

### **REVIEW OF IMMUNOASSAY-BASED BIOSENSORS**

#### **1.1 INTRODUCTION**

Biosensors are analytical tools that are used widely in the food industry, clinical diagnostics, agricultural fieldwork, and biomedical research. Research in this area is focused toward advancing the detection modalities commonly used for signal monitoring. Because of the vast amount of research in this area, our focus in this project is on affinity-based biosensors that exploit antibody-antigen interaction with the aim of implementing a sensitive detection modality. Biosensors based on antibody-antigen interactions are commonly referred to as immunoassay-based sensors, or immunosensors. Common immunoassay detection modalities rely on charged couple device technology as well as surface plasmon resonance methods for antibody-antigen detection. To that effect, I intend for this project to provide another detection modality that is optically based with high sensitivity and that can be interfaced directly with antibody. In this chapter, I provide an overview about research efforts being made on immunoassay-based biosensors, namely on the detection modality and the immobilization of protein to the sensor. In addition, I present some examples of commercial biosensors and outline our approach for designing an immunoassay-based biosensor.

## 1.2 OVERVIEW OF BIOSENSORS

Biosensors are analytical devices composed of a detecting element and a transducer. The detecting element can be molecular or cellular based components such as enzymes, antibodies, or whole cells such as bacteria (Reviews [1-3]). The transducer element can be based on a charge-coupling device (CCD), photodiodes, surface plasmon resonance, or quartz crystal microbalance (QCM). With the exception of QCM, all mentioned transducers are optically based techniques while QCM is based on gravimetric measurement, which monitors the mass variation of a quartz chip due to the adsorption of protein from solution onto the sensor surface. An illustration of a typical biosensor design is shown in figure 1.1.

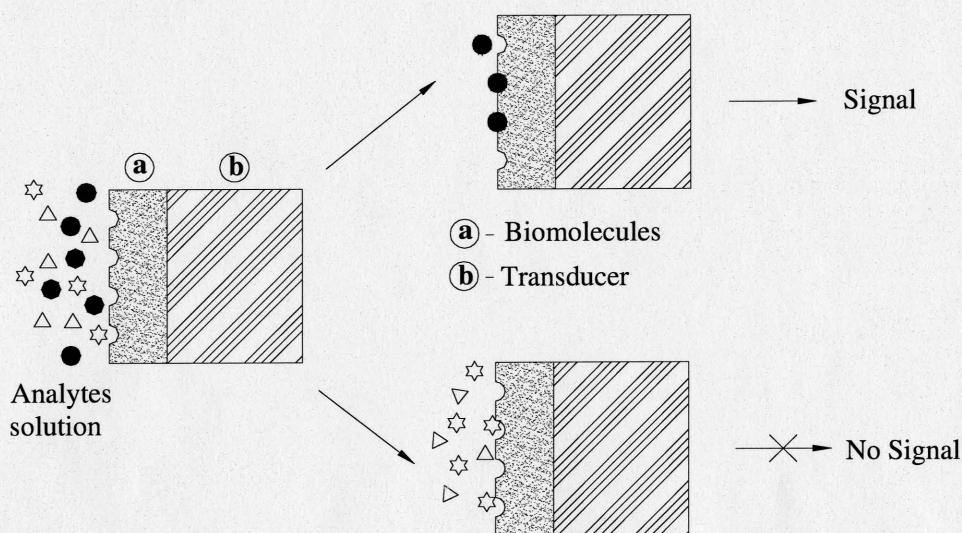


Figure 1.1 – Components of a typical biosensor. As depicted, specificity is a key property for a biosensor. (Redrawn from M. Keusgen [4]).

As figure 1.1 illustrates, the design of a biosensor requires the integration of the biomolecules with the detection element. A reliable biosensor is a device that produces



low false positive signal and is able to detect minute (nanomolar-picomolar) amounts of target molecules being measured. False positive readout is the result of the non-specificity of the probe in the biosensor to multiple targets. Often we look at the probability of having a false readout and the intent is to minimize such probability. A curve known as the Receiver Operation Characteristics (ROC-curve) describes the change in sensitivity of a biosensor with the false positive readout. In addition, specificity is inherent in the affinity of the biomolecules to its target. On the other hand, sensitivity is mostly based on the ability of the transducer to measure a signal that is the result of a minute amount of the target. In the following paragraphs, a discussion on the type of biomolecules and transducers used is presented.

Biomolecules often used in biosensors can be enzyme, DNA, antibody, cellular receptor, aptamer<sup>1</sup>, whole cells and so on [4-7]. Enzyme-based biosensors are widely used and one commercial example is the Abbot-Medisense® blood glucose meter. Glucose oxidase is immobilized on the sensing surface and the measurement is based on the oxidation of glucose in the blood catalyzed by the enzyme. Electrons generated from the oxidation-reduction reaction create a current which is a function of the glucose level in the blood [1].

Antibodies are used in this project due to their ubiquitous use as biomarkers in clinical research. Antibodies are proteins produced mainly by B cells of the immune system against specific biomolecules or small molecules referred to as antigens. The generation of antibody for clinical research and diagnostics has been mostly based on the

---

<sup>1</sup> Aptamers are nucleic acid sequences synthetically designed with biochemical properties resembling those of antibodies, namely aptamers can be specific to proteins or small molecules.

monoclonal antibody technology (hybridoma cell) developed in 1975 by Kohler and Milstein [8]. Briefly, the specific antigen is injected into a host (e.g. mouse, goat, or rabbit) leading to an immunogenic response. Antigen-specific plasma cells are isolated from the host and fused with cancerous cells creating hybrid cells. Monoclonal antibodies are then purified using chromatography techniques from hybrid cells. The advancement of recombinant technology has paved the way for new techniques such as phage display or ribosomal display whereby a large library of antibodies can be designed. Indeed, the generation of antibody through phage display has been done and the process is cheaper and less time consuming than monoclonal antibody technology. However, purification and selection of specific antibody can be a laborious process [5]. At least 10,000 antibodies are available commercially. Antibodies are classified into five class families based on the type of heavy chains. I have used immunoglobulin G (IgG) in this project. One difference between IgG and the rest of all immunoglobulins is based on the type of heavy chain used or the number of antigen binding sites. A typical structure of an IgG antibody is shown in figure 1.2.

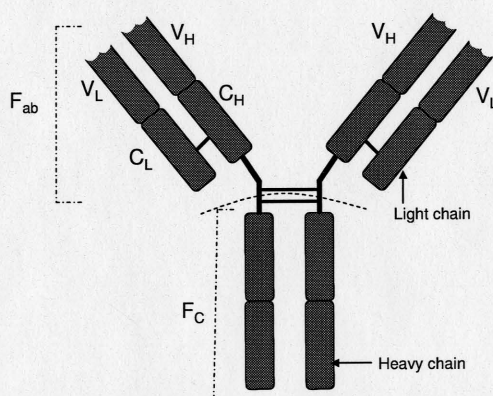


Figure 1.2 – Structure of an IgG. Shown are the variable and constant domains. Variable chains ( $V_H$  and  $V_L$ ) form the antigen binding site.

As depicted, each antibody is composed of two heavy chains, linked by disulfide bonds, and within each heavy chain there are four proteins domains (one variable domain ( $V_H$ ) and three constant domains ( $C_H$ )). There are two light chains in an IgG structure and each light chain is composed of two protein domains (a variable domain ( $V_L$ ) and a constant domain ( $C_L$ )). Each light chain is linked to a heavy chain via a disulfide bond. The variable portions ( $V_H$  and  $V_L$ ) of the antibody structure form the antigen-binding site, which there are two sites for an IgG. The antibody can be cleaved using proteolytic enzymes such as pepsin or papain creating at least two fragments commonly referred to as the  $F_{ab}$  (antigen binding fragment, which can be mono- or divalent depending on the enzyme used) and an  $F_c$  portion (crystallizable or constant fragment) [3].

Functionally, the antibody is designed to recognize its cognate protein, i.e. antigen. One of the hallmarks of antibodies is their high binding affinity to their antigen. However, antibodies may be cross-reactive – the ability to recognize multiple antigens of similar chemical structures – which remains an issue. In the context of biosensors, antibody cross-reactivity results in a false positive readout. Antibody-antigen interactions are often associated with affinity constants that describe the tight binding of the antigen. The sensitivity of antibody-based biosensors is rather high indicated by the low value of  $K_M = 10^{-18}$  that can be achieved. In other words, picomolar concentration of antigen in solution can be detected using antibodies.

As mentioned earlier, immunoassays are techniques based on antibody-antigen affinity used for the detection of antigen in solution. One of the most common immunoassay used



in screening for specific antigens is enzyme-linked immunosorbent assay (ELISA). Typically, target molecules (hereafter analyte(s)<sup>2</sup>), either immobilized on a solid substrate or dissolved in solution, are detected using functionalized antibodies. An illustration of common immunoassay techniques is shown in figure 1.3.

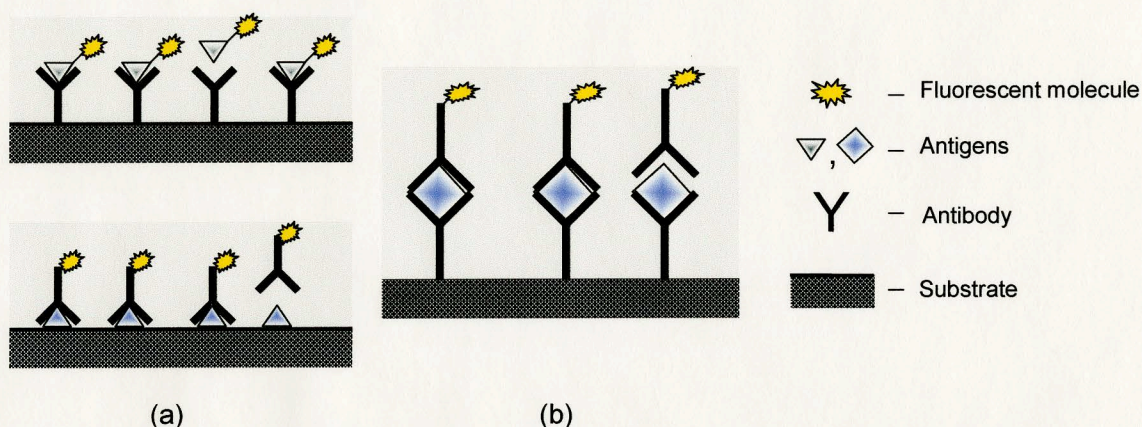


Figure 1.3 – Immunoassay techniques. A generic immunoassay is shown in panel (a) while a sandwiched immunoassay is depicted in panel (b). Antibody as well as antigen can be tagged with fluorescent molecules.

Depending on the type of immunoassay, antibodies or antigens can be conjugated with fluorophores (e.g. Cy5 (red), Cy3 (green), FITC (green), Rhodamine conjugated fluorophores, etc), radioactive elements, or enzymes such as peroxidase. The visualization of antibody recognition of its cognate is done using fluorescent microscopy, autoradiography film, phosphoimager, or Forster resonance energy transfer methods [5, 9]. Following a calibration curve, the intensity of fluorescent light generated is a function of the concentration of the analyte in solution.

<sup>2</sup> I use the term 'analyte' instead of 'antigen' in immunoassay-based sensor as analytes can be more general since an antigen can be a protein, small molecule or even an antibody. Hence the use of analytes to avoid confusion

The use of immunoassay with a detection method constitutes the immunoassay-based biosensor being sought. The specificity of this sensor is governed by the biomolecules on the surface of the transducer element. The immobilization process is critical to the function of the antibody. Indeed, surface chemistry of the substrate has long been thought to affect the activity of the protein adsorbed on the surface of solid substrates [10]. The chemical nature of a surface affects the orientation of antibody as well as the amount of protein adsorbed to the surface of the substrate [11-13]. The choice of surface chemistry and therefore the immobilization process of probe molecules will have an effect on the sensitivity of the immunoassay-based microdevice. In the forthcoming section, surface chemistry of the substrate is discussed.

### **1.3 PROTEIN IMMOBILIZATION**

The immobilization of antibody to the surface of the transducer is a crucial step in the design of a biosensor as such step affects the orientation of the protein resulting in changes to the sensitivity of the biosensor [5, 11-13]. Here an overview of the surface modifications that has been of great use in immunoassay-based biosensors is presented. My intention is to present examples of surfaces and surface effects on the adsorption of antibody. This section contains a glimpse of what has been accomplished in surface chemistry for biosensors application. I limit the discussion to mostly surface modifications of silicon substrate, as there has been a plethora of information on modifying gold-based surfaces commonly used in surface plasmon resonance technique. In addition, our design of an immunoassay-based biosensor involves a silicon substrate. The adsorption capacity of proteins on bare substrates is lower than on chemically

modified substrates [5]. Veisich et al. [14], using surface plasmon resonance technique, showed that the amount of proteins was higher on modified sensor surface than on bare sensor surface. In addition, control of protein adsorption such as orientation of antibodies can be controlled with chemical functionalization of substrates instead of bare substrates [11]. Therefore, the chemical modification of the surface of biosensors, discussed in the next section, is a prerequisite for protein attachment.

### 1.3.1 SURFACE CHEMISTRY EFFECT ON PROTEIN ADSORPTION

Coating compounds that self-assemble to form mono- or multi-layer (SAMs) thin films have been designed to immobilize antibodies via physical adsorption, non-covalent, or covalent attachment. Self-assembly has been widely used due its ease of implementation and low cost. Examples of chemicals used in self assembly are 3-aminopropyltriethoxysilane (APTES), 3-aminopropyltrimethoxysilane (APTS), aminophenylsilane (APhS), 3-glycidoxypropyltrimethoxysilane(GPTS), 3-mercaptopropyltrimethoxysilane (MPTS), and many more [15, 16]. Some SAMs compounds are shown in figure 1.4.

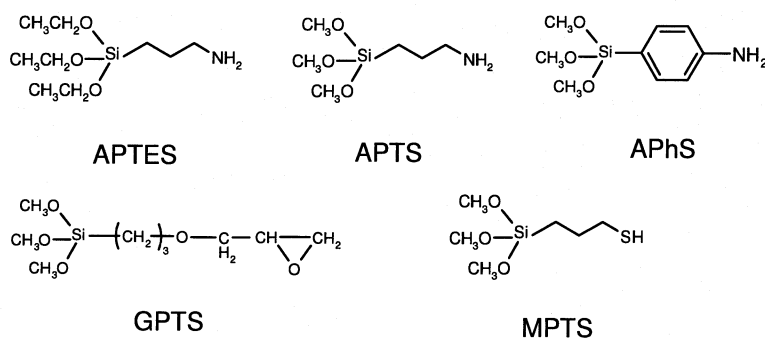


Figure 1.4 – Chemical structures of common silane compounds.

Zhang *et al.* studied the surface coverage of silicon oxide film by APTS and APhS [13]. They found that solution parameters such as concentration of monomers, time of immersion, temperature, and water content affect the surface capacity of amine present on the surface. In turn, the surface coverage of amine groups will affect the binding capacity of the monolayer for antibodies. X-ray photoelectron spectroscopy and atomic force microscopy were used to analyze the molecular characteristics of the amino-based silane coatings. It was found that APhS resulted in high surface coverage compared to APTS. In addition, water content changed dramatically the morphology of the silane film, which altered the binding capacity of amine-terminated surfaces. Other studies on APTES have confirmed that solution parameters previously mentioned drastically controlled the surface chemistry and morphology of APTES. For highest surface amine content, Zhang *et al.* proposed a low concentration of APTS as well as a time of incubation of 5 hrs. Vanderberg *et al.* [17] and Akkoyun *et al.* [18] in their studies on APTES showed that low monomer content but longer time of incubation (longer than 5 hours) are needed for increasing the surface coverage by amino groups. The low concentration of monomer needed for good surface coverage has been demonstrated for mercaptopropyltrimethoxysilane (MPTS). Hu *et al.* [19] showed that good self-assembly of MPTS occurred at monomer concentration of 5 mM above which surface morphology, characterized by surface roughness, was increased. Overall, these studies highlight the effects of solution conditions on the coating films of substrates used in protein immobilization.



In their study on alkanethiol, Li and co-workers [12] studied the adsorption behavior of proteins on Carboxyl (COOH) terminated and methyl (CH<sub>3</sub>) terminated SAMs. The effect of temperature during the preparation of SAM was shown to affect the amount of lysozyme adsorbed on the surface. COOH-terminated SAMs prepared at 50 °C exhibited higher amount of adsorbed lysozyme in comparison to COOH-terminated SAMs prepared at 22 °C. On the other hand, methyl terminated SAMs showed similar protein adsorption characteristics independent of temperature. That is in line with many studies that showed proteins tend to have higher affinity to hydrophobic surfaces. Further evidence of the effect of surface chemistry on protein adsorption was illustrated by Chen *et. al.* [11]. Amine terminated and carboxyl terminated coatings on silicon oxide were created and the orientation of antibody on each surface was monitored using surface plasmon resonance. Antibody orientation was dependent on surface characteristics as antibody adsorbed on NH<sub>2</sub>-terminated substrate exhibited either side-on or end-on orientation, i.e. the antibody- binding site is exposed to the bulk solution. On the other hand, antibodies adsorbed on COOH-terminated surfaces were head-on orientated, i.e. Fc portion is exposed to the solution. A scheme illustrates antibody orientation on different surface chemistry shown in figure 1.5.

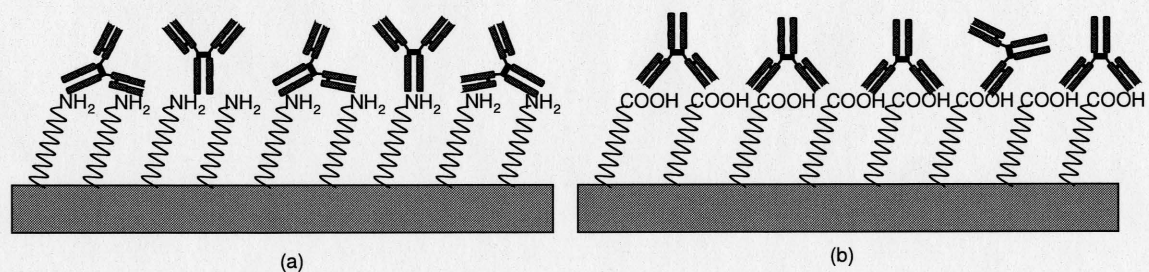


Figure 1.5 - Effect of surface chemistry on antibody orientation. (Redrawn from Chen *et. al.*)



In immunoassay, end-on orientation is most preferred (Fc is down), as the sensitivity of the technique is unchanged because antibody-binding site is in proximity to antigen solution. Another effect of surface chemistry, as demonstrated in figure 1.5, is the type of interaction between the protein and the functional group of the surface. Overall, surface chemistry does affect the amount of adsorbed protein, the orientation of protein on the surface, and their activity. In the next section, I present a few methods used for attachment of antibodies.

### **1.3.2 IMMOBILIZATION METHODS FOR IMMUNOASSAY**

I just described how surface chemistry could affect the adsorption of protein on solid substrate. This will have an effect on the sensitivity of the immunoassay-based biosensors by 1) determining the amount of antibody on the surface and 2) determining antibody functional orientation. Now the question is how we immobilize the antibody on the sensor surface. Numerous examples of antibody immobilization methods are readily available. For instance, silicon oxide surfaces coated with APTES have been widely used for immobilizing antibody. However, antibody attachment to APTES is unstable as the pH of the solution is varied. In order to provide more stable attachment, amine terminated surfaces can be further modified to provide a covalent attachment of antibody. Using ethyl-3-[1-dimethylamino-propyl] carbodiimide (EDC) and N-hydroxysuccinimide (NHS) allows the covalent attachment of proteins. This method allows the covalent attachment of antibody via an  $\text{NH}_2$  group on the antibody [14, 18, 20]. In addition, 3-glycidoxypolytrimethoxysilane (GPTS) has been used to immobilize protein on the

surface of glass. The epoxy group on the GPTS compounds provides a more stable attachment, covalent, of antibody to the substrate. Shin *et al.* [21] have used GPTS to covalently immobilize proteins on glass substrate.

Another common method used to immobilize antibody on the surface using strong noncovalent binding is based on avidin-biotin interaction. Usually streptavidin or neutravidin is immobilized on the substrate creating an avidin layer. The avidin coating will serve as linker for antibody attachment via coupling of biotinylated-antibody. This method has been implemented in patterning antibody for immunoassay applications [18, 22-27]. For instance, Taitt *et al.* [23] in their study on detection of *Salmonella* spp., a food pathogen, immobilized anti-salmonella antibody on the sensor surface via the avidin-biotin approach. Streptavidin was immobilized on the glass substrate and biotinylated anti-*Salmonella* spp. was linked to avidin, thereby immobilizing the antibody to the substrate.

Midwood *et al.* [28] developed a new method for covalently attaching antibody on oxide layer of silicon substrate. The covalent attachment of antibody is accomplished using silicon samples coupled to phosphonate coating incubated in disuccinimidyl glutarate (DSG). Fluorescent measurement indicated the presence of rabbit antibody on phosphonate-coated silicon substrate.

So far, I have presented some examples for materials used to immobilize protein on silica-based substrates. For high throughput screening, typically high-density protein arrays are needed. The latter task can be accomplished using numerous protein patterning methods, which are discussed in the following section.

#### 1.4 PROTEIN PATTERNING FOR IMMUNOASSAY

As mentioned previously, immobilization of antibodies onto solid surfaces is a critical step toward integrating biomolecules with solid-state devices in the design of biosensors. In immunoassay, antibodies or analytes are typically arrayed in a matrix form to increase surface density and screen for multiple targets. Protein patterning is done on planar substrates that were modified with one of the chemistries discussed previously. Microliters to nanoliters of protein solution are typically used. The exposed area of the samples, whereby proteins were not immobilized, has to be passivated to reduce the non-specific adsorption of target molecules and improve immunoassay biosensor function. To prevent nonspecific adsorption, numerous chemical schemes have been developed. I stress that a universal surface treatment that resists adsorption of all proteins is not available. Rather, protein-resistant surfaces are tailored toward the type of proteins for which nonspecific adsorption is needed. In their effort to provide a guideline for making protein resistant surfaces, Ostumi *et al.*[29] have indicated that surfaces should have the following conditions: (1) surface is hydrophilic, (2) surface molecules should include hydrogen acceptor groups, (3) surface molecules should be void of hydrogen donor groups, and (4) overall surface charge is neutral. It is worth mentioning that these criteria should not be all satisfied to design protein-resistant surface. For example, Lee *et al.* [30] has reduced the nonspecific binding of proteins by coating a surface with a hydrophobic film based on fluorinated carbon which has the trademark name CYTOP. Lee *et al.*[30] showed that the application of CYTOP to silicon-based substrate reduced the background noise of the fluorescent signal due to nonspecific binding of proteins.

One of the popular methods used and studied for its passivation capability utilizes bovine serum albumin (BSA) [31, 32]. The use of BSA as a passivation layer is common in immunoassay techniques. Other examples of protein-resistant surfaces include polyethylene glycol surfaces, which have been demonstrated to reduce nonspecific protein adsorption in studies by Veiseh *et. al.* and Shin *et. al.* [14, 21]. In addition, carbohydrate layers such as chitosan and dextran have been studied to understand the nonspecific binding for IgG and lysozyme [18, 21]. All these biomolecule-based and polymer-based coatings used for reducing nonspecific protein adsorption share a common feature: they are highly hydrophilic. Having discussed the methods used for reducing nonspecific adsorption, the objective at this stage is directed toward high-density protein patterning methods.

Several protein-patterning techniques have been developed for high density protein microarrays for immunoassay biosensors. Photochemical method [21, 33], microcontact printing ( $\mu$ CP) [34], microfluidic network ( $\mu$ FN) [32], and spotting or spraying [35] are techniques used for proteins patterning some of which are summarized in figure 1.6.

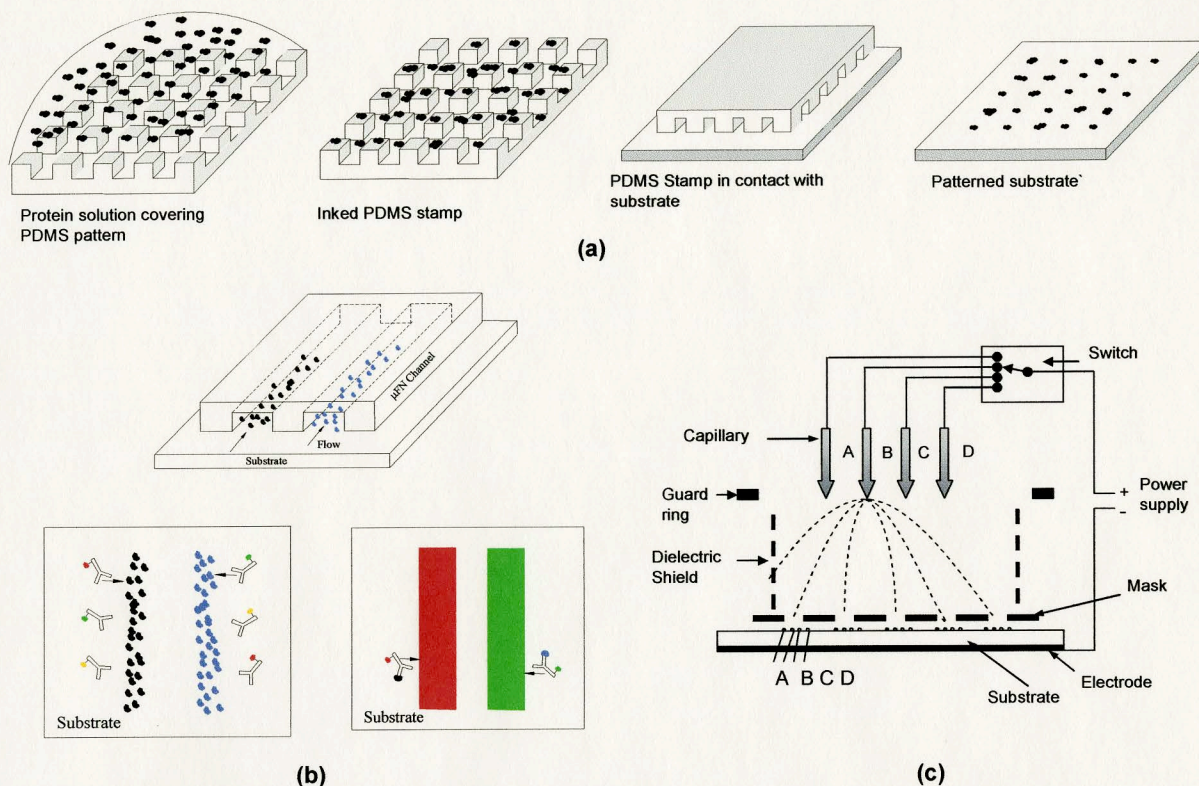


Figure 1.6 – Microcontact printing (a), microfluidic network (b), and electrospray deposition (c) are shown. For detailed description, refer to text. (Redrawn from refs. [32, 34, 35]). Several steps are needed to form a protein microarray using microcontact printing as shown in panel (a). In panel (b), the immobilization of antibodies using microfluidic methods requires the flow of antibody solution and removal of microfluidic channels thereafter. Antibody-patterned substrate is incubated in fluorescently labeled antibodies. Fluorescent microscopy is used to image the substrate. Electron spray deposition technique is shown in panel (c).

Although not illustrated in figure 1.6, photochemical methods rely on photolabile molecules to pattern a protein. The use of UV energy in the patterning of protein can be detrimental to the function of the protein, therefore limiting the ability of this technique. Microcontact printing is a technique developed by Whitesides at Harvard University intended to pattern curved substrates. Briefly, a polydimethylsiloxane (PDMS) mask is fabricated using photolithographic method and then incubated in a protein solution. Proteins are adsorbed to the PDMS mask and excess proteins are washed away using a



buffer solution. The protein-loaded PDMS mask is then placed in contact with a substrate that will allow proteins transfer from PDMS mask to a substrate creating a protein pattern. Renault *et al.* [34] have used microcontact printing ( $\mu$ CP) to print protein patterns onto glass substrates but the patterns lacked uniformity as shown in panel (a) of figure 1.6. Microfluidic network ( $\mu$ FN) is another protein patterning technique commonly used. This method, like  $\mu$ CP, uses a microchannel system made of PDMS elastomer fabricated using photolithography. PDMS-based channels are placed in contact with a substrate (gold, silica) and protein solutions are flowed through channels. Excess proteins are removed using a buffer solution rinse and microfluidic channels are lifted away from the sample. Patterned substrates are immersed in a blocking solution such as BSA. The presence of protein can be tested using an immunoassay technique. Delamarche *et.al.* [32] showed that the substrate and the elastomer are tightly sealed through spontaneous adhesion of PDMS elastomer to glass substrate. Analytes such as chicken IgG and mouse IgG were immobilized onto chemically functionalized glass substrates. Antibody-coated substrate was incubated in a solution containing Cy3-labeled anti-chicken IgG and Cy5-labeled anti-mouse IgG antibody to validate the presence of analytes. Fluorescent imaging microscopy was used to analyze the samples. Panel (b) of figure 1.6 indicated that cross-reactivity did not take place as separate green and red colored lines were observed. This study illustrated the potential use of  $\mu$ FN as a patterning technique for immunoassay-based biosensor. The other technique depicted in panel (c) of figure 1.6 is electrospray deposition (ESD) developed by Morozov *et al.* [35]. ESD has been developed to pattern several proteins onto solid surfaces. This technique uses capillary

tubes to hold different protein solutions that are to be printed. Protein printing is done sequentially and a movable mask is used to create the pattern on the substrate. As depicted in the panel (c) of figure 1.6, the charged protein in the capillary follow a path that is maintained by the field created (between electrode and capillary) as well as the dielectric shield. One of the drawbacks of this technique is the loss of the activity of proteins being printed upon impact with the substrate [35]. Another method for patterning protein is based on microarray spotting which has shown great potential for immunoassay applications. Hence, a review of papers describing the use of microarray techniques for application in immunoassay-based biosensors, namely protein microarray, will follow.

#### **1.4.1 MICROARRAY PATTERNING FOR IMMUNOASSAY**

Protein patterning using microarray technology has great potentials for immunoassay-based biosensors. Microarray technology has been used widely for high throughput screening in genomic research and clinical diagnostics [9]. High-density protein microarrays should have around 10,000 spots per 25mm x 75 mm glass slide. The setback of using microarray for proteomics (study of the physiologic state of the cell at the protein level) is related to the lower functional stability of protein compared to DNA. In other words, retention of biological activity in the nanoliter volume of protein spotted on a glass slide must be sustained [5]. Surface modification of the glass slide along with optimized printing and solution conditions such as temperature, humidity, and ionic strength of buffer allow the design of functional protein microarrays. To that effect, I present some examples of using microarray technology for patterning proteins.

Microarray printing is usually performed using an automated arrayer consisting of capillary pins. Contact and noncontact modalities are used to transfer protein solution from capillaries on to modified glass slides [27]. In the former modality, capillary pins come in direct contact with the substrate where the latter modality uses piezoelectric<sup>3</sup>-based capillary pins to transfer protein solution onto glass substrate. Other venues of spotting microarray protein, though less popular, have previously been discussed such as ESD [27, 35]. I wish to discuss the use of microarray for immunoassay applications as has been demonstrated by several authors.

Michaud *et al.* [36] used microarray technique to print about 5000 yeast proteins on modified glass slides in order to study antibody specificity to such proteins. Their result showed the potential use of microarray for screening antibody against specific antigen in a high throughput scheme. However, cross-reactivity of antibody was observed as certain antibodies were able to recognize multiple antigens, though with variable signal intensity. Macbeath *et al.* [37] also used protein microarray to study protein G and IgG interaction as well as other protein-protein interactions. On a modified glass substrate, quadruplicate of three different proteins, one of which was protein G were printed using a microarray printer. ProteinG-IgG interactions were validated using fluorescent microscopy techniques that indicated the presence of fluorescing spots due to proteinG interaction with IgG. The data were also an evidence that protein G retained its activity on the modified glass substrates used in the study by MacBeath and co-workers. In another study on microarray, Haab *et al.* [38] examined antigen-antibody interaction using 115

---

<sup>3</sup> Piezoelectric materials have the ability to undergo mechanical deformation when placed under a voltage source. Mechanical deformations of capillary lead to compressing the solution within the pin leading to ejection of droplets.



antibodies and their corresponding 115 antigens. In one set of experiments, the author spotted microarray of 115 antigens, each antigen was spotted 6-12 times. The antigen microarray was then immersed in a solution of 115 fluorescently labeled antibodies (two-color scheme) solutions. Fluorescent microscopy was used to image all protein microarray slides and quantitative analysis was performed. Although cross-reactivity was observed for certain antibodies, the author identified antibodies and their cognates for half the number of antigens spotted on the glass substrate. This study (Haab *et al.*) is a good example of the potential use of microarray technique for immunoassay-based microensing. In a study to identify the presence of cholera toxin in a solution, Delehanty *et al.* [26] used noncontact microarray printing to immobilize anti-cholera toxin antibody on glass substrate. Antibody coated substrates were immersed in a Cy5-labeled cholera toxin and detection was done using a fluorescent scanner. Recognition of cholera toxin was observed indicating the specificity of anti-cholera antibody to its cognate protein.

All of these studies highlight the potential use of microarray technology for immunoassay in clinical diagnostics or drug screening. As such, microarray technology will be an invaluable tool in developing a high throughput immunoassay-based biosensor.

## **1.5 IMMUNOASSAY-BASED BIOSENSOR**

Having described the importance of the surface chemistry on protein adsorption, protein immobilization methods, and protein patterning techniques, I provide, in this section, a holistic view of immunoassay-based biosensor. Some examples of immunoassay methods that have been used in clinical diagnostics, screening antibody specificity, and food

industry will be described. The focus is directed more toward the transducer component of immunoassay-based biosensor.

Moremo-Bondi *et al.* [39] have designed an antibody-based biochip whereby antibodies are printed on a nylon membrane and photodiodes are used as detector elements. Specifically, anti-sheep IgG and anti-mouse IgG were immobilized on a nylon membrane in quadruplicates. Rabbit IgG was used as a control and Cy5-labeled solutions of mouse IgG and sheep IgG were added first separately, then in a mixed solution to the nylon membrane. The biochip employed a laser source to excite fluorescently labeled antibodies immobilized to a nylon membrane. As a detection element, Photodiodes were used to acquire fluorescent signals. Results indicated that photodiodes were able to detect the signal from each antibody spot and distinguish differences between control and experimental samples. In addition, no cross-reactivity of antibodies was observed. In a similar setup, Askari *et al.* [40] used the antibody-based biochip with the sensing element being the photodiode array to detect protein p53, a tumor suppressor protein. Monoclonal p53 antibody was spotted onto nylon membrane, which was then incubated in a Cy5 labeled p53 protein solution. In order to verify that photodiode can detect multiple targets in solution, goat anti-IgG was immobilized to the nylon membrane. The photodiode was able to detect the multiple targets in solution. In a clinical diagnostic aspect, a series of anti-p53 antibody was added to human sera, which were spotted on the nylon membrane. Using their immunoassay, photodiodes were able to detect signals representing p53 presence in human sera. It should be mentioned that the nylon membrane whereby antibodies were printed was not physically linked to the photodiode

array. Instead, an optical lens system was needed to focus the fluorescent signal emanating from the nylon membrane onto the photodiode system. In our biosensors, as described later, the intent is to print proteins directly on the photodetectors.

Taitt *et. al.* [23] as well as Yu *et. al.* [25] have used immunoassay-based biosensors for detecting the presence of *Salmonella* spp. and *E. coli.* in food samples. Taitt and co-workers used a multianalyte array biosensor to detect the presence of *Salmonella* spp. Different analytes were immobilized on modified glass waveguides using the microfluidic network ( $\mu$ FN) method described earlier. A light source was coupled into a waveguide to generate an evanescent wave capable of exciting Cy5 fluorophore conjugated to antibodies used in the detection assay. The imaging was done using a CCD. Taitt *et. al.* were able to detect the presence of salmonella, using the multianalyte immunosensor, in spiked food samples. In a similar study to detect food pathogen, Yu *et. al.* employed a different immunoassay-based biosensor. Their system used functionalized magnetic beads on which antibodies were immobilized to probe the presence of target samples. The detection principle was based on electrochemiluminescence using a commercial photomultiplier tube. As demonstrated, immunoassay-based biosensors can be used as analytical tools for screening pathogens in food samples. Surface Plasmon Resonance (SPR) technique is by far the most widely used commercial immunoassay-based biosensor. It has been used in a wide spectrum of areas such as in food industry, clinical diagnostics, protein-protein interaction studies and so on. Therefore, I wish to present some examples of commercial biosensors that employ SPR technique.

### 1.5.1 EXAMPLES OF COMMERCIAL BIOSENSORS

My focus in this section is to present examples of commercial biosensors while keeping to the theme of the project, immunoassay-based microdevices. To that effect, the focus is on commercial biosensors that employ immunoassay techniques.

Most commercial biosensors are based on the platform developed around the early 90's by Biacore Instrument (Sweden). The Biacore instrument, based on surface plasmon resonance (SPR), became the first commercial optical biosensor used for biomolecular analysis [41]. These systems have been used in drug discovery studies, food monitoring, environmental studies, and biomolecular research [42]. In addition, new SPR-based biosensors were introduced to the commercial market of biosensors.

The Biacore instrument relies on the surface plasmon resonance technique. Briefly, the detection process is as follows: antibodies are immobilized on the gold surface of the Biacore structure and a solution of analyte is flowed through an elastomeric channel. An optical detector monitors the change in refractive index via changes in the angle of reflected light due to the formation of antibody-analyte complexes in solution. The following scheme shown in figure 1.7 provides a better visualization of the Biacore system [4, 6, 43].

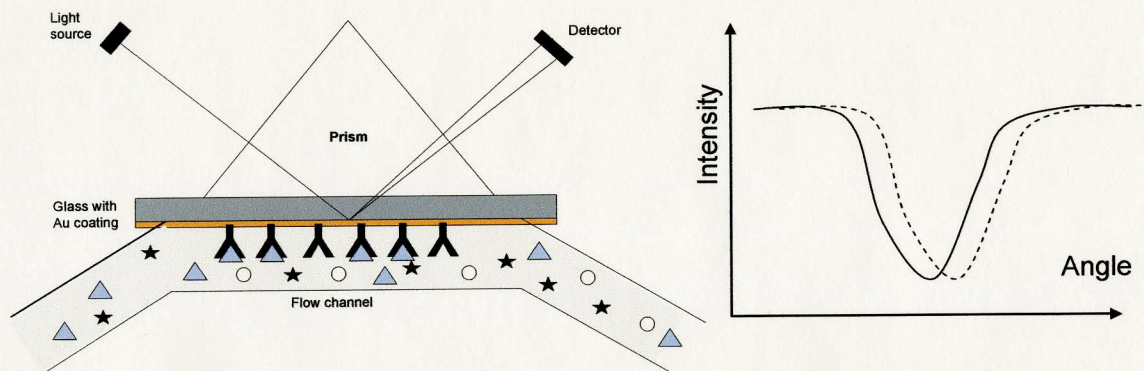


Figure 1.7 – Principle of SPR detection. As the light source strikes the metal surface of the glass substrate, surface plasmon wave is emanated from the gold material. Difference in the angles of reflection is related to the formation of antibody-antigen complexes in solution.

Other commercially available biosensors developed by IAsys<sup>®</sup> Instrument, Nippon Laser Electronics, Texas Instruments, and IBIS Technologies are also SPR-based biosensors. These sensors are modified versions of the Biacore platform including user-friendly configurations in terms of software use, sampling, and reusability through UV/ozone cleaning [41]. In addition, miniaturized optically based biosensor has been designed as the device developed by Texas Instruments, Spreeta<sup>®</sup>, offer the maneuverability needed for fieldwork application. Despite all the advances in Biacore platforms, cost remains an issue as well as the requirement for large hardware components. Current research, e.g. the present work, is focused on the integration of immunoassays with microelectronic devices for the development of low cost and effective biosensors. High throughput analysis is a desired design specification and microelectronic devices based on complementary-metal-oxide-semiconductor (CMOS) technology are well suited for this purpose. With that in mind, this work is focused on the integration of antibody with solid-state detectors, namely avalanche photodiodes introduced in chapter 3.

## 1.6 SUMMARY AND PROPOSED BIOSENSOR DESIGN

The design of immunoassay-based microdevice requires the integration of several components for producing a sensitive, specific, and low cost device.

1. Surface chemistry affects the adsorption of protein and that the stability of antibody immobilized on a surface can affect the sensitivity of the device. In addition, surface chemistry alters the orientation of antibodies on substrates.
2. Covalent immobilization of antibody on the surface of biosensors, accomplished using approaches discussed in this chapter, provides stability for the biosensor in case of a pH change.
3. The presence of target molecules is confirmed using labeled solution of tagged antibodies or tagged target molecules. The detection of analytes can be based on fluorescent or chemiluminescent signals. Unlike fluorescence whereby an excitation source is needed, chemiluminescence is emitted from a chemical reaction. The decay of chemiluminescence is longer than fluorescence, hence the preference for using chemiluminescence in this project. The detection modalities for either fluorescence or chemiluminescence are based on autoradiography films, fluorescence microscopy, photodiodes and so on.
4. The integration of surface chemistry, antibodies, and detection modalities will lead to designing an immunoassay-based biosensor.

Hence, these issues will be considered in the design of an immunoassay-based microdevice. In the section on immunoassay biosensor, with the exception of SPR, most techniques did not exhibit on-chip readout; that is the detector element acquires the signal



from antibody without employing additional element. With respect to SPR, the availability of such technique is hindered by the high cost of the Biacore platform. To that effect, I have combined the specificity of immunoassay techniques with the high sensitivity of avalanche photodiode in the prospect of designing a biochip with on-chip readout. The ability to perform single photon detection makes avalanche photodiode a desirable and wise choice as our sensor element. The immunoassay-based microsensor will also be low cost and portable for fieldwork applications.

In the following chapter, the attachment of antibody to the oxide layer of silicon substrates is presented along with results on the characterization of the coupling agent and on protein attachment. Immunoassay techniques are used to validate the presence of protein on the oxide layer of silicon substrates.

## CHAPTER 2

### ANTIBODY ATTACHMENT TO FUNCTIONALIZED SILICA SUBSTRATES

#### 2.1 INTRODUCTION

We have seen in the literature review that surface chemistry of substrate affects the adsorption of biomolecules, the orientation and the activity of the protein. In addition, the immobilization method for antibody is critical for the stability of the protein in case of pH change. I have used silicon-based substrate with an oxide layer to perform the attachment of antibody. In choosing a coupling agent, I have focused on using silane-based compounds as their use for immunoassay based biosensor have been demonstrated [12, 18, 21]. In addition, silanization is an easy process, low cost, though can be time consuming. The characterization of surface coating using infrared spectroscopy and atomic force microscopy was also performed. Following surface modification and characterization, either mouse anti-human collagen type IV or mouse anti-biotin antibody was manually spotted onto the modified silicon substrate. I have used an immunoassay similar to ELISA to detect the presence of antibody on the surface or detect the presence of biotin in solution. At this step in designing the immunoassay-based microdevice, I have relied on autoradiography film. Mouse anti-human collagen type IV retained its activity as radiography images showed. In addition, mouse anti-biotin antibody was active on the substrate as radiography film indicated the recognition of biotin in solution. In this chapter, experimental results on surface modification, surface characterization as well as on biomolecules attachment are presented. Demonstrating the ability to attach



antibody onto modified oxide layer of silicon substrate will be step closer to the integration of biomolecules with the detection element. The proposed approach for our immunoassay-based microsensing design is depicted in figure 2.1.

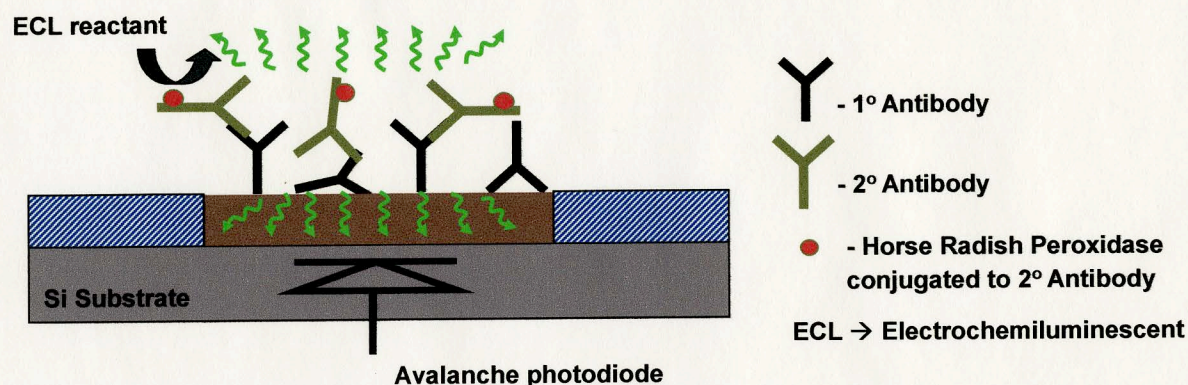


Figure 2.1 – Proposed design for a portable, on-chip readout immunoassay-based sensor.

## 2.2 SUBSTRATE MODIFICATION

In this section, sample preparation as well as the characterization of functionalized substrates will be discussed. First, the procedure for substrate preparation is presented.

I have used silane compounds namely glycidoxypolytriethoxysilane (GPTS). GPTS is a known adhesive in the metal coating industry [44]. The silanization of GPTS follows a three-step mechanism as was proposed by McGovern *et. al.* in their study on Octadecyltrichlorosilane (OTS) [45]. The silanization mechanism for GPTS may resemble the mechanism of OTS involving a hydrolysis step (i.e. formation of silanetriol by hydrolyzing the  $\text{—OCH}_3$  groups on GPTS), followed by adsorption of the silanetriol onto the substrate forming  $\text{Si—O—Si}$  bonds. Antibody immobilization using GPTS

provides a covalent linkage between the sensor surface and biomolecules. The attachment of antibodies using GPTS is more stable compared to using APTES, which provides noncovalent attachment of biomolecules [5]. The epoxy group on GPTS coated surface reacts with an amino group on the protein as figure 2.2 shows.

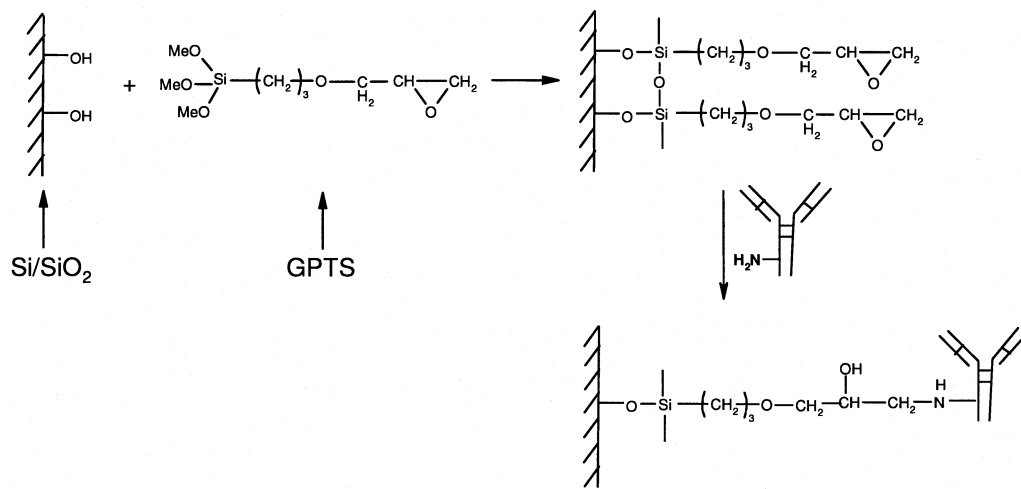


Figure 2.2 – A scheme for antibody attachment on GPTS coated silicon substrate. The silanization process occurs via a three-step mechanism as explained in the text. Regarding antibody attachment, any amine group on the antibody could react with the epoxy group on the substrate, although the location of NH<sub>2</sub> on the antibody as shown here is more desirable for our immunoassay.

Avalanche photodiodes, i.e. detection element, are based on silicon substrate. Therefore, silicon based substrates were used on which an oxide layer was grown using thermal oxidation technique to facilitate chemical attachment of GPTS. Silicon (Si) substrates (4 in<sup>2</sup>) were cleaned in a piranha solution (1:5 v/v H<sub>2</sub>O<sub>2</sub>:H<sub>2</sub>SO<sub>4</sub>) for 10 min. and immersed in a concentrated hydrofluoric acid (HF) solution to etch away surface coatings. Si samples were blown dried with N<sub>2</sub> and placed in an oven for oxidation. Thermal oxidation was done for 1 hr, which resulted in an estimate oxide layer thickness of 500 nm. Following thermal oxidation, Si samples were cooled and few samples were selected

to measure the thickness of the oxide layer using an optical interference technique. On average, a thickness of 0.5  $\mu\text{m}$  thin film of oxide was observed. Oxidized Si substrates were then diced into 1 in.<sup>2</sup> samples and cleaned in 1:5 ( $\text{H}_2\text{O}_2\text{:H}_2\text{SO}_4$ ) piranha solution for 10 min. This was followed by a thorough DI  $\text{H}_2\text{O}$  rinsing and immersing the samples in 1:100 HF solution for 1 min. It is thought that the dilute HF cleaning will increase the amount of hydroxyl group on the oxide surface, thereby increasing the immobilization capacity of the surface. A thorough DI  $\text{H}_2\text{O}$  rinsing followed the dilute HF treatment. Samples were dried under a stream of  $\text{N}_2$  and were stored in a desiccator under vacuum prior use.

Silicon substrates (1in<sup>2</sup>) were immersed in 2% (v/v) solution GPTS in hexane for 5hrs with agitation. The previous conditions were determined from FTIR characterization. Following, GPTS-coated substrates were rinsed twice with hexane and twice with acetone. The substrates were dried with a stream of  $\text{N}_2$  and were used immediately for protein attachment. Prior to introducing the procedure of antibody attachment to the GPTS-coated silicon substrates, I present the characterization of the surface coating.

## 2.3 GPTS COATING CHARACTERIZATION

In characterizing APTS coating of silicon substrates, Zhang *et al.* studied the effect of solution parameters on surface coverage and morphology which has been shown to affect protein adsorption [12]. X-ray photoelectron spectroscopy was used – a technique based on the interaction of x-ray with a material, capable of performing elemental composition of the surface – to determine the  $\text{NH}_2$  coverage of the surface. XPS data are displayed in terms of signal intensity versus photoelectron energy, corresponding to each element on

the surface such as N, C, O, and so on. I have followed in similar footsteps of this study, i.e. characterization of surface and morphology, for GPTS coating. The characterization of GPTS with XPS would not be suitable, as the amount of oxygen atoms within a 0.5  $\mu\text{m}$ -thick oxide layer far exceeds the amount of Oxygen within the epoxy ring of GPTS monomers. Instead, Fourier Transform Infrared Spectroscopy (FTIR) was used to characterize the presence of epoxy groups on the oxide layer of the silicon substrates. Regarding GPTS, the presence of epoxy and methyl group as shown in its molecular structure would be used to identify the presence of GPTS coating on the surface.

I have focused on studying the effect of monomer concentration and time of incubation on the coverage and surface chemistry. The coating process was done in a similar fashion as the preparation of silicon done previously. The samples in this case were prepared differently because the FTIR configuration used was in a reflection mode. Specifically, I have used reflection-absorption infrared spectroscopy (RAIRS) configuration to characterize qualitatively the presence of epoxy group on substrates. Nicolet Magna IR, 50 Spectrometer, Series II<sup>®</sup> was used for FTIR measurements. Solution conditions used to prepare the samples are summarized in table 1.

Table 1 – Experimental conditions for FTIR experiment.

Parameter: Time			Parameter: GTS Concentration		
Time (hrs)	[GTS] (% in hexane)	Water (% v/v)	Time (hrs)	[GTS] (% in hexane)	Water (% v/v)
2	2	< 0.01	5	0.2	< 0.01
5	2	< 0.01	5	2	< 0.01
8	2	< 0.01	5	4	< 0.01
12	2	< 0.01	5	8	< 0.01

As mentioned, samples used for the FTIR study were not based on silicon; instead, I have used glass substrates that were coated with a thin film of gold (Au). Thin films of silica were grown on Au and were plasma cleaned prior to the acquisition of background silica. Sample preparation and FTIR analysis are summarized in figure 2.3.

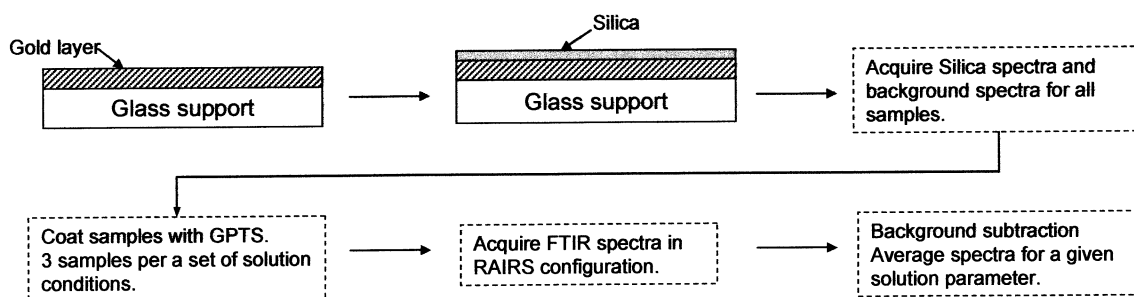


Figure 2.3 – Flow chart for FTIR measurements and analysis.

FTIR spectra for silica background and neat GPTS on KBr pellets were acquired. The presence of a SiOSi peak in the FTIR spectrum shown in figure 2.4 showed that gold thin films were coated with Silica.

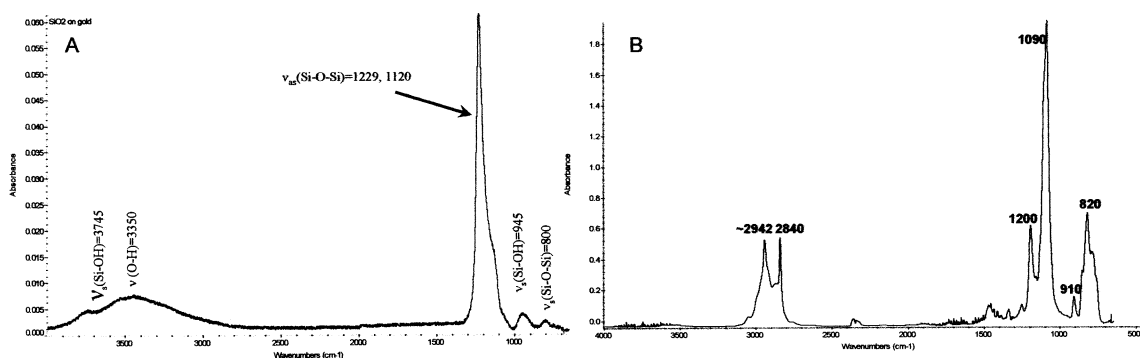


Figure 2.4 – FTIR spectra for silica grown on gold and neat GPTS on KBr pellets. The silica presence on Au layer is indicated by the strong SiOSi vibration. For GPTS, the absence of SiOCH<sub>3</sub> shown around 820 on silicon will indicate the presence of the coating.

The 'neat' GPTS spectrum shown in panel (b) of figure 2.4 indicates the presence of the epoxy group at  $910\text{ cm}^{-1}$  and the presence of Si-OCH<sub>3</sub> vibrational mode around  $820\text{ cm}^{-1}$ . In coating silica layer with GPTS, we expect the strong FTIR signal around  $820\text{ cm}^{-1}$  to decrease. GPTS coating was done in a glass Petri dish for each solution condition (3 samples). All samples were plasma cleaned for 2 min 30 sec prior immersion into GPTS solution. The incubation time and GPTS concentration were chosen as indicated in table 1. Substrates coated with GPTS were stored in a desiccator prior to FTIR analysis. FTIR data for time and concentration effects on GPTS coating of silica layer are shown in figure 2.5. Each FTIR spectrum shown here is the average of three measurements.



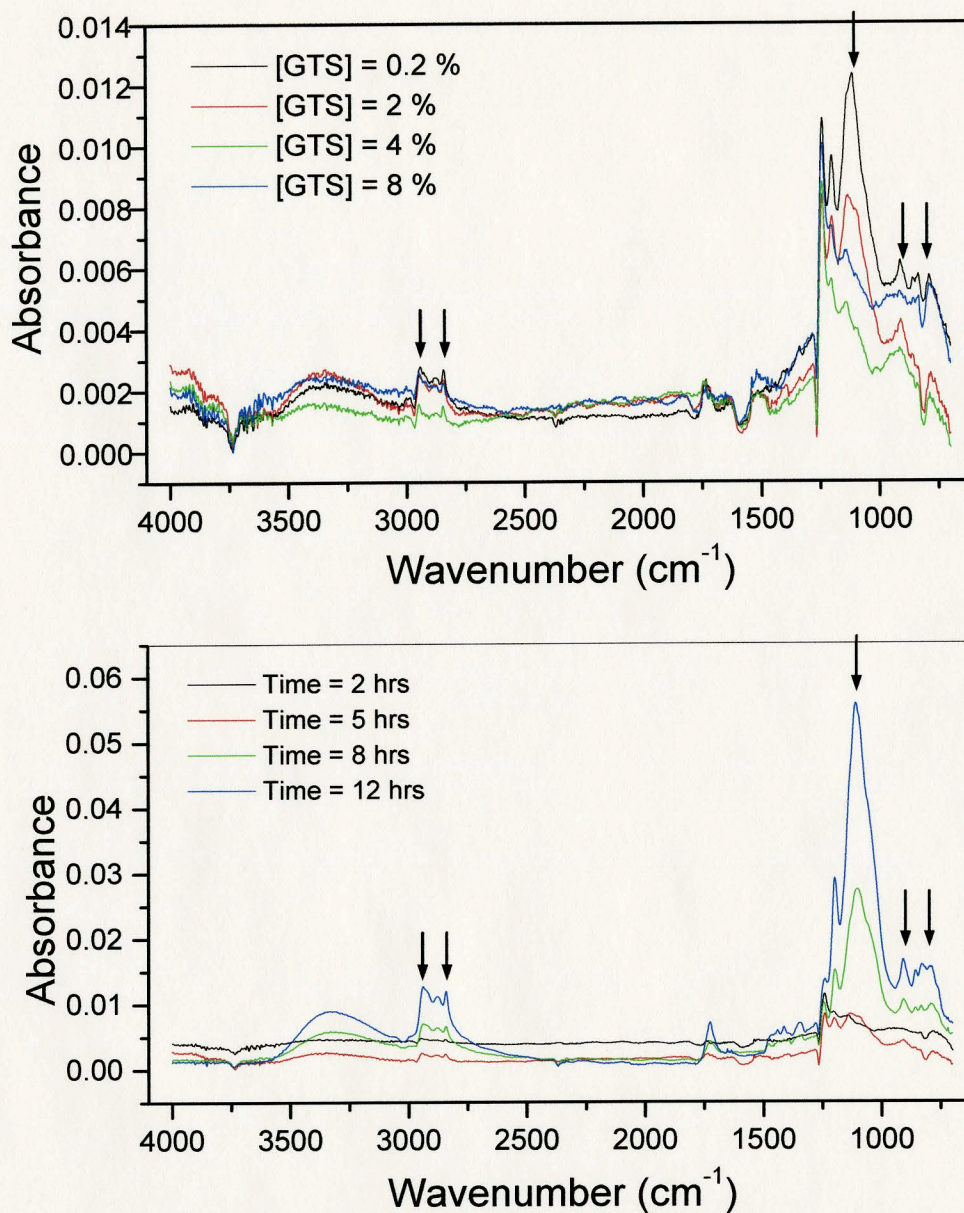


Figure 2.5 – FTIR data on GPTS coated substrates. Time and concentration variations are illustrated. Spectra shown for each solution condition are the average of three replicates.

Concerning the FTIR data, the signals of interest are indicated by arrows shown in figure 2.5. Epoxy vibrational frequency occurs around  $910 \text{ cm}^{-1}$  (second arrow from the right in figure 2.5) clearly indicating the presence of GPTS on the surface. In addition, the



decrease in the signal corresponding to  $\text{SiOCH}_3$  vibration is apparent in figure 2.5. This clearly indicates that GPTS reacted with the hydroxyl groups on the oxide layer grown on gold. Another indirect indication for the GPTS coating is the Si-O-Si bond peak around  $1100\text{ cm}^{-1}$  and the C-H vibration in the range of  $2840\text{--}2940\text{ cm}^{-1}$ . The other signal shown in figure 2.5 represents the vibrational frequency for hydroxyl (OH) vibration. The incubation time for silica-based samples in GPTS coating varied from 2 hrs up to 12 hrs. It is clearly observed around  $910\text{ cm}^{-1}$  that longer time will increase the amount of epoxy group on the surface. In terms of concentration of GPTS monomer, less than 2% GPTS solution is desirable for good surface coverage. This is in agreement with data published in the literature on APTES, APTS, and MPTS [13, 17-19]. High concentration of silane monomers in solution results in the polymerization of the silane in the bulk reducing the amount of  $\text{SiOCH}_3$  for reaction with oxide layer. From these findings, a time of 5hrs and a 2% GPTS concentration in hexane was used in subsequent work.

Atomic force microscopy (AFM), a surface imaging technique, was used to study the surface morphology of GPTS-coated oxide layer of silicon samples. Specifically, tapping mode-AFM was used to image the surface of GPTS-coated substrate and measure surface roughness. Samples in this case were  $0.25\text{ in}^2$  Si/SiO<sub>2</sub> prepared as follows: oxidized silicon substrates with  $1\text{ in}^2$  surface area were diced into  $0.25\text{ in}^2$  samples to fit in the instrument. The newly cut samples were cleaned as described previously for coating GPTS for  $1\text{ in}^2$  samples. Cleaned oxidized silicon substrates ( $0.25\text{ in}^2$  surface area) were then immersed in a 2% GPTS solution for a time of 5hrs with varied water concentration. AFM analysis was performed following the coating of the samples. Scan areas of  $0.25$

$\mu\text{m}^2$  and  $0.25\text{ nm}^2$  were imaged for a background sample (cleaned Si/SiO<sub>2</sub>) and GPTS-coated Si sample. AFM images obtained using Dimension 3100 AFM<sup>®</sup> (Digital Instrument, Veeco Metrology Group) with scanning areas of  $0.25\text{ nm}^2$  are summarized in figure 2.6.

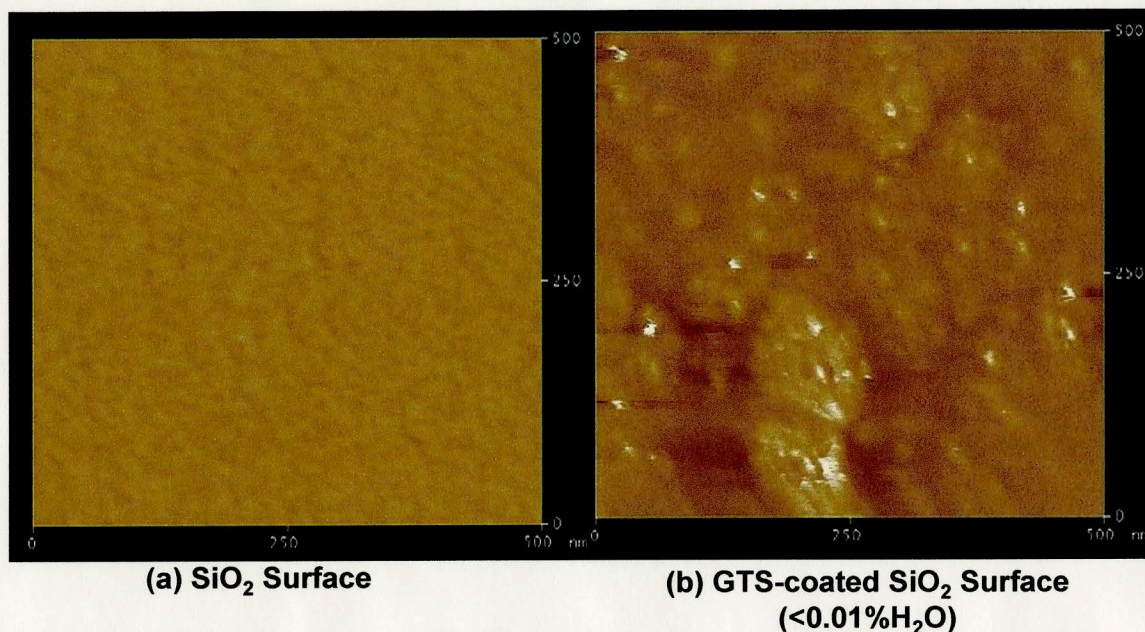


Figure 2.6 – AFM images of bare SiO<sub>2</sub> and GPTS-coated silicon oxide layer. The roughness of SiO<sub>2</sub> and GPTS coating were 0.120 nm, and 0.245 nm, respectively.

The roughness values in this case were 0.12 nm and 0.245 nm for SiO<sub>2</sub> and GPTS-coating, respectively. In panel (b), aggregated structures of GPTS, which are characteristic of self-assembly of silane compounds, are observed.

Having determined the reaction condition for GPTS coating for oxide layer of silicon substrates, antibody attachment was performed on modified samples. The presence of antibody on substrates was determined using an immunoassay technique.

## **2.4 IMMUNOASSAY MEASUREMENTS**

In this section, a description of the protein attachment procedure is presented followed by immunoassay data on antibody attachment to GPTS-coated silicon substrates. In addition, the activity of the antibody on the surface was determined using an assay based on the interaction between Mouse anti-biotin IgG and biotin conjugated to HRP.

### **2.4.1 EXPERIMENTAL PROCEDURE**

A solution of 1:500 Mouse anti-human collagen type IV IgG (1° Ab) dissolved in phosphate saline buffer (PBS, pH ~ 7.4-7.7) was spotted using a micropipette on the chemically modified silicon substrates. A total number of 25 spots per sample were printed with a 0.3 µl Ab solution per spot. Silicon samples were incubated in the 1° Ab for 30 minutes. Substrates were rinsed in PBS and immersed in 2% (w/v) BSA solution for 30 min. The rinsing step was repeated and the samples were transferred to a 1:10,000 anti-mouse IgG secondary antibody solution and incubated for 1 hour. Following another rinsing step in PBS, the samples were immersed in the chemiluminescent substrate solution following the manufacturer protocol (MichDiag, Rochester MI). Autoradiography film was exposed to the sample for various time intervals. Experimental steps used for the immobilization of proteins and the detection of chemiluminescence are shown in figure 2.7.



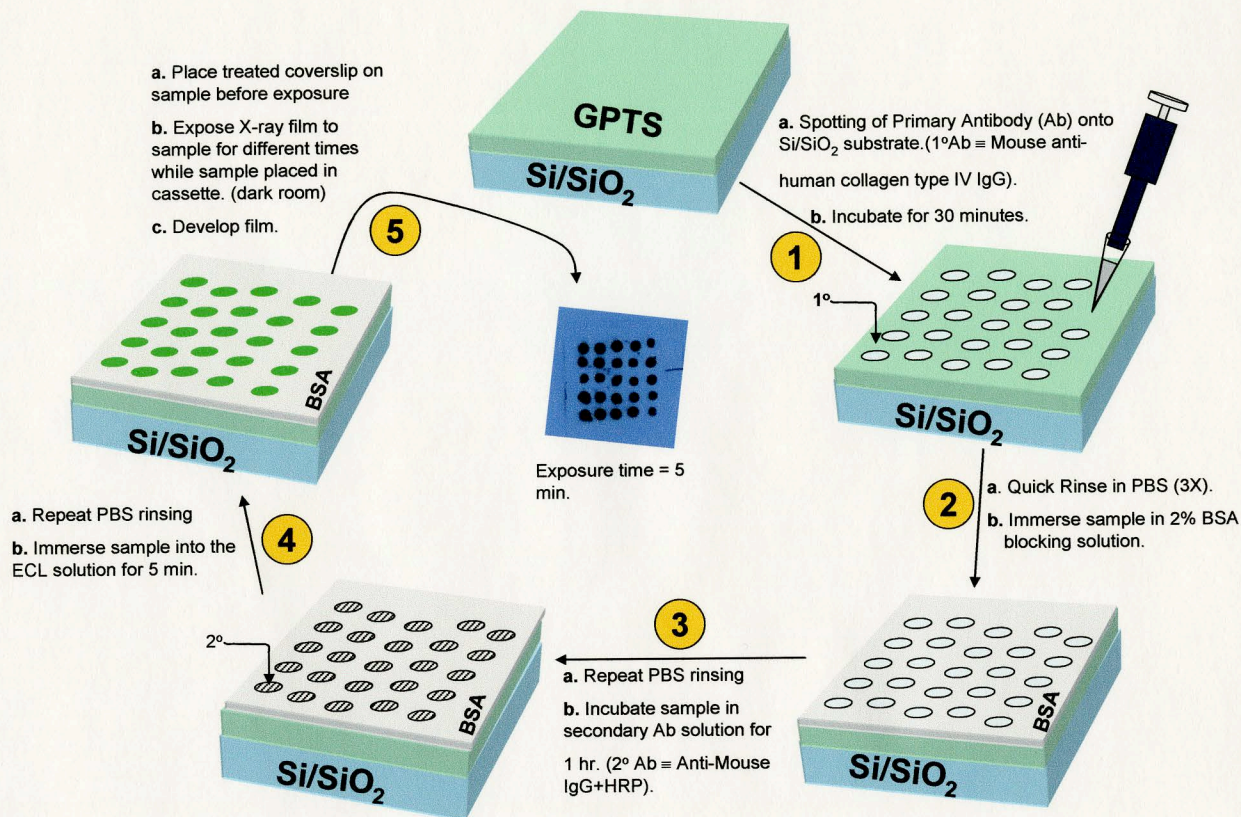


Figure 2.7 –Immunoassay protocol used in antibody attachment and detection. A radiography image of one experiment is depicted in the center of this scheme.

The chemiluminescence is generated from the reaction of an organic chemiluminescent substrate such as luminol or dioxetane substrate with horseradish peroxidase (HRP) conjugated to the secondary antibody. The reaction between Luminol and HRP in the presence of an oxidant ( $O_2$  or  $H_2O_2$ ) results in blue light emission. An example of chemiluminescence generation is shown in figure 2.8.

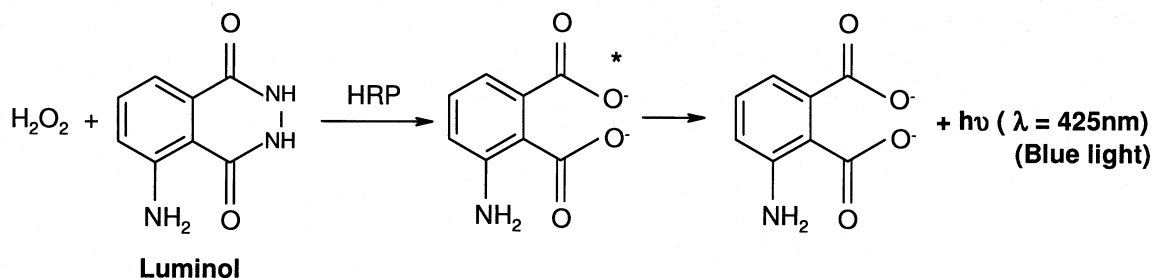


Figure 2.8 - Generation of chemiluminescence through reaction between an organic substrate (luminol) with peroxidase. In this case, visible but dim blue light is emitted. (\*) indicates an excited state emitter).

The intensity of chemiluminescence depends on the concentration of the enzyme, the substrate (i.e. luminol), peroxide as well as the presence of enhancer molecules. In this study, I have followed the manufacturer protocol in preparing the chemiluminescent substrate. In-depth discussion on the methods and mechanisms for generating chemiluminescence can be found elsewhere [46-48].

In the experimental scheme shown in figure 2.7, step 5 of the immunoassay is important for obtaining a good radiography image. In other words to reduce nonspecific adsorption of the secondary to the coverslip, the latter was coated with GPTS hence reducing background noise often seen in autoradiography images.

## 2.4.2 RESULTS AND DISCUSSION

Mouse anti-human collagen type IV IgG ( $1^\circ$  Ab) was printed onto a GPTS coated silicon substrate. The presence of  $1^\circ$  Ab on the substrate was verified using a chemiluminescence tracer within the immunoassay procedure. A control experiment was done to verify that the presence of spot on the radiography image is not due to the nonspecific adsorption of the anti-mouse IgG conjugated to HRP to the substrate. The control measurements consisted of printing  $0.3\ \mu\text{l}$  spots of PBS buffer. In this case, the immunoassay shown in



figure 2.7 was repeated. The data for control and experimental measurements are summarized in figure 2.9.

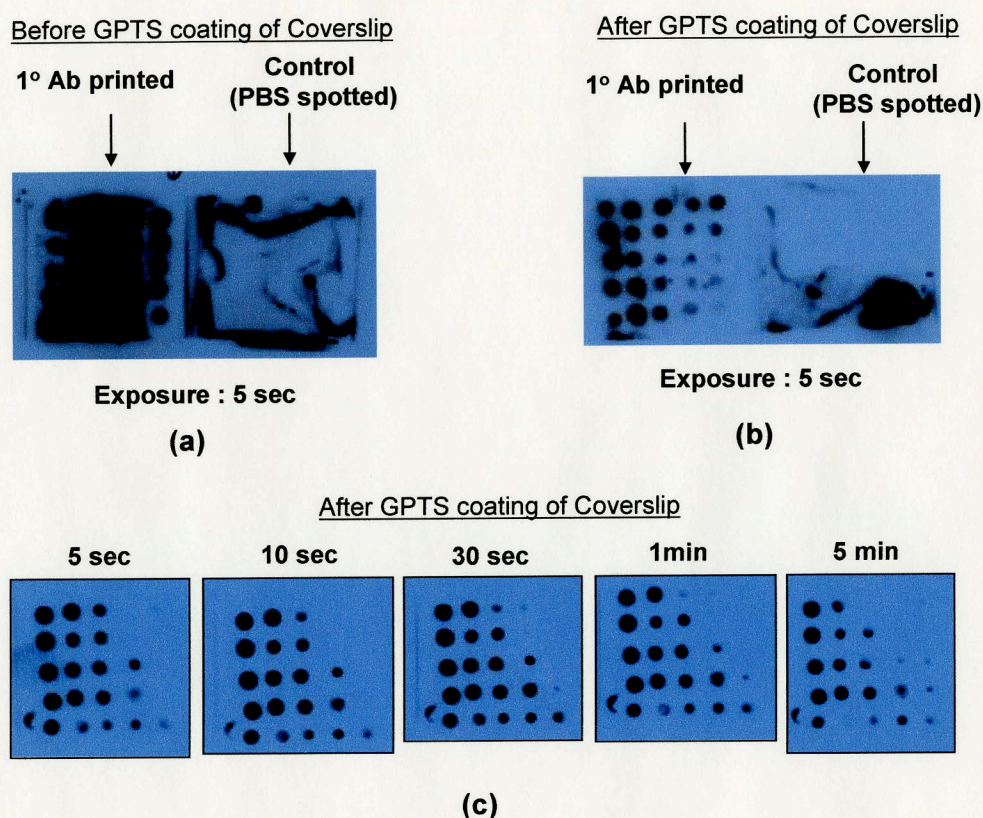


Figure 2.9 – Data on primary antibody attachment to the GPTS-coated silicon oxide layer.

As shown in figure 2.9, the treatment of coverslip with GPTS reduced the background noise observed in panel (a). The antibody array printed onto modified silicon substrates with GPTS-treated coverslip (panel (b)) is easier to distinguish in the radiography image than with untreated-coverslip (panel (a)). The chemiluminescence detected is due to the 1° Ab–2° Ab interaction and not due to the nonspecific adsorption of the secondary antibody on the modified silicon substrates. A series of exposure of the radiography film

to the substrate is shown in panel (c). The background noise is totally reduced and positive signals are observed. However, missing spots are noticed as well as variability in the diameters of Ab spots. The antibody array was manually spotted using a micropipette, which is not a very accurate method for printing. An automated arrayer should be used to reduce the variability in spot diameters. The missing spots may be due to the nonhomogenous coating of the rather large substrate ( $1\text{in}^2 \sim 6.45\text{ cm}^2$ ). Typically, the size of substrates used for silanization in the literature is about  $1\text{ cm}^2$ . Nonetheless, GPTS allowed the immobilization of antibody to the oxide layer of silicon substrates.

A dosage experiment using the radiography techniques was performed. Briefly, four solutions of  $1^\circ$  Ab were printed on GPTS coated substrate. The dilution factors used were 1:50, 1:2500, 1:125000, and  $1:3.75 \times 10^6$  (micromolar to nanomolar concentration). Autoradiography are not sensitive techniques, therefore, detecting almost picomolar range concentration of Ab was not possible. The presence of antibody on the surface was validated using the immunoassay used previously. Figure 2.10 presents results of the dosage experiment.



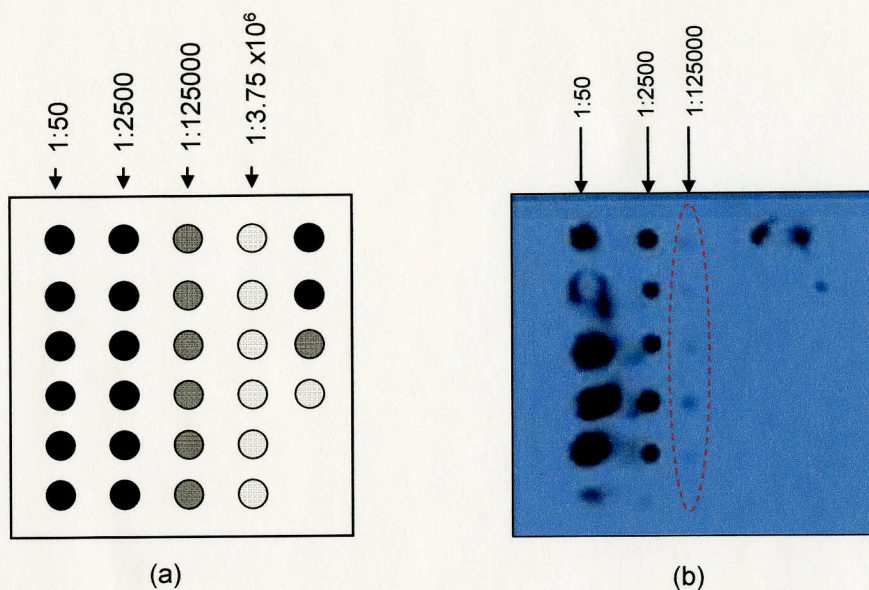


Figure 2.10 – Dosage experiment. Four dilution factors were used in the preparation of 1<sup>o</sup> Ab solutions. The template shown in panel (a) was followed during the spotting of antibodies solutions. The results of the dosage experiment are shown in panel (b).

A template of the spotting strategy of the 1<sup>o</sup>Ab solution is depicted in panel (a). As shown in panel (b) of figure 2.10, I was able to observe nanomolar concentration of the 1<sup>o</sup> Ab immobilized on the surface. The concentration for 1:125000 1<sup>o</sup> Ab solution was estimated from the optical density of 1:50 1<sup>o</sup> Ab solution.

Up to this point, I have shown that mouse anti-human collagen type IV IgG (1<sup>o</sup>Ab) can be immobilized to GPTS-coated silicon substrates. The presence of 1<sup>o</sup> Ab was verified using an immunoassay based on chemiluminescence detection. Although anti-mouse IgG conjugated to HRP detected the presence of 1<sup>o</sup> Ab surface, the activity of antibody as it pertains to its binding ability, was not demonstrated. Therefore, an immunoassay based on anti-biotin IgG and HRP-tagged biotin interaction was used with anti-biotin IgG immobilized on the GPTS coated surface. The orientation of the anti-

biotin IgG will affect the bioactivity of the antibody, i.e. an active anti-biotin IgG on GPTS coated surface will have its  $F_{ab}$  portion exposed to the biotin solution.

A series of dilutions for anti-biotin IgG was prepared in PBS. Using a pipette, 0.3  $\mu$ l spots from each solution were spotted on GPTS-modified silicon substrates. The purpose for doing such measurement is to 1) determine a working dilution for mouse anti-biotin IgG and 2) study the bioactivity of anti-biotin IgG on GPTS-coated substrates. A template for the spotting procedure for anti-biotin IgG is shown in panel (a) of figure 2.11. Subsequent steps were similar to the immunoassay described in figure 2.7 with few exceptions. For instance, the step where a secondary antibody solution is added is replaced with a solution of 1:2000 of HRP-tagged biotin prepared from a 0.75 mg/ml stock solution. Coverslips were treated with GPTS to reduce background noise. The results of this experiment are shown in figure 2.11. Radiography images shown in panels (b) and (c) are for different time intervals.



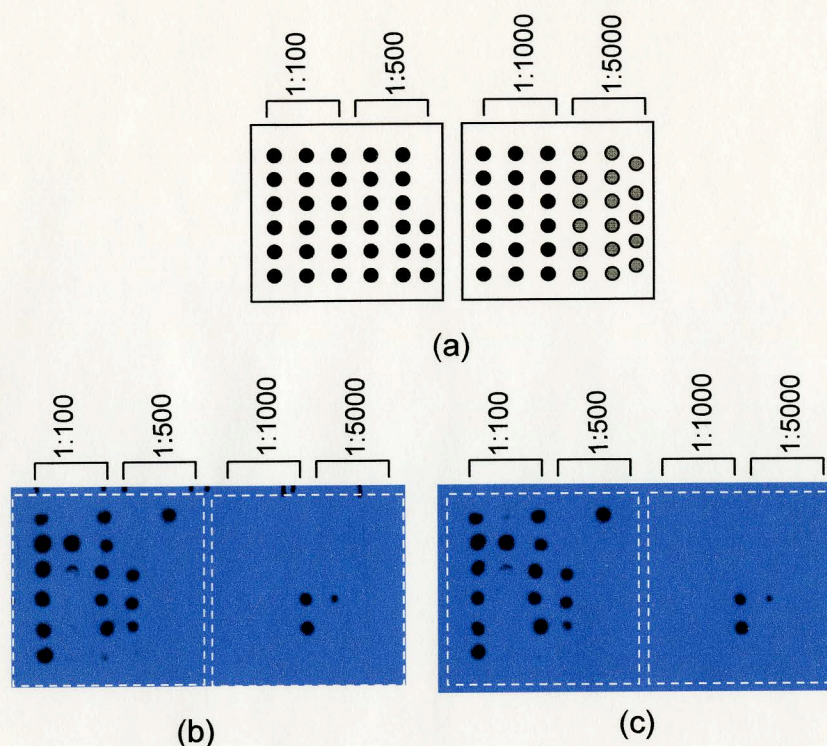


Figure 2.11 – Mouse monoclonal anti-biotin IgG printed on GPTS-coated silicon dioxide in 1:100, 1:500, 1:1000, and 1:5000 dilution factors in the pattern shown in panel (a). Panels (b) and (c) depict radiography images of the assay to detect biotin conjugated to HRP.

Spots shown in panels (b) and (c) are due to interaction between anti-biotin IgG and biotin conjugated to HRP. Clearly, anti-biotin IgG immobilized onto GPTS modified substrates retained its activity. For subsequent measurements a 1:100 dilution factor was chosen for spotting anti-biotin IgG onto GPTS-coated silicon substrates.

In another set of experiments, anti-biotin IgG was arrayed in a similar fashion as shown in figure 2.7 on GPTS coated substrates. After a blocking solution, antibody-coated substrates were immersed either in a 1:2000 biotin conjugate to HRP solution (prepared from a biotin stock solution of 1mg/ml) or in a PBS solution. The latter solution (i.e. PBS) serves as ‘control’ measurement. The results from these experiments are shown in figure 2.12.



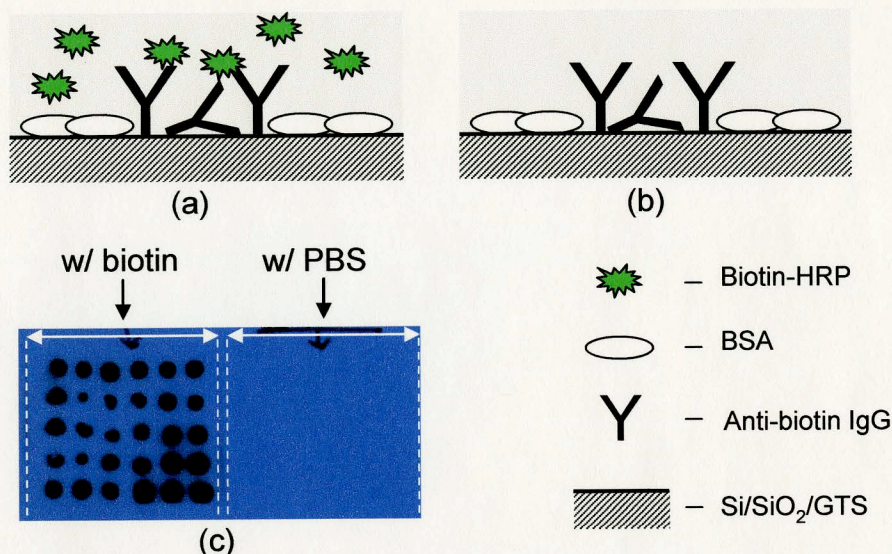


Figure 2.12 – A 1:100 Mouse anti-biotin IgG was printed in a 6x5 array on two 1 in<sup>2</sup> GPTS coated silicon oxide layers. One sample was immersed in a biotin-HRP solution while another sample was immersed in a buffer solution as shown panels (a) and (b). As expected, no signal was observed for panel (b).

In panel (c) of figure 2.12 (w/biotin), positive signals shown indicate that anti-biotin IgG is active on GPTS-coated substrates. In other words, HRP-tagged biotin is able to bind to the antigen-binding site of the anti-biotin IgG. For the ‘control’ measurements, the absence of chemiluminescence signals was expected as the anti-biotin coated substrate was incubated in a PBS solution free from HRP-tagged biotin. In fact, no chemiluminescent signal was observed as indicated in panel (c) of figure 2.12 (w/PBS).

## 2.5 SUMMARY AND CONCLUSION

In this chapter, I have shown using Infrared spectroscopy and Atomic force microscopy that glycidoxypyltrimethoxysilane (GPTS) was bound to the oxide layer of silicon

substrates. GPTS-coated substrates were immobilized with analytes in array format (mouse anti-human collagen type IV IgG) to determine the attachment of proteins to GPTS. Using a tracer antibody (HRP-tagged anti-mouse IgG) solution, I was able to confirm, via the detection of chemiluminescence, that GPTS-coated substrates retained the analytes. Nonspecific adsorption of the HRP-tagged anti-mouse IgG to the GPTS-coated substrate was verified using a 'control' experiment with PBS buffer spotted instead of primary antibody. The activity of Mouse anti-biotin IgG immobilized on GPTS-coated substrates was verified using an immunoassay with an HRP-tagged analyte. Anti-biotin IgG coated silicon substrates were able to recognize the presence of HRP-tagged biotin in a buffer solution. This was an indication that the antigen-binding site of anti-biotin IgG was exposed to the surface, i.e. Fc-down orientation. Having determined the solution parameters as well as verified the antibody attachment, antibody was coupled to the transducer surface in an effort to build an immunoassay-based microdevice. The following chapter contains data on the integration of antibody with a detection modality.

## **CHAPTER 3**

### **TOWARD AN IMMUNOASSAY-BASED BIOSENSOR**

#### **3.1 INTRODUCTION**

Mouse anti-biotin IgG and Mouse anti-human collagen type IV retained their biological activity when immobilized onto GPTS coated surface as immunoassay results indicated. In developing an immunoassay-based biosensor, the coupling of biomolecules to the transducer surface must be performed. Immunoassay techniques will be used to validate the presence of antibody on the transducer; however, the detection modality is now based on avalanche photodiodes instead of radiography films. In this chapter, I describe the detection modality used, the coupling of antibody to the avalanche photodiode, and present data on APD detection of chemiluminescence light. First, a short review on the principle of avalanche photodiode and operation will be described.

#### **3.2 BACKGROUND ON AVALANCHE PHOTODIODES**

Current readout systems in the area of immunoassay-based biosensors involve the use of CCD techniques, autoradiography techniques, for labeled analytes. Although CCD techniques are good imaging techniques, slow response time in switching is one drawback [49]. Avalanche photodiodes (APDs) were chosen as they offer superior photon sensitivity (possibility of single-photon detection), fast switching time, and compatibility with complementary-metal-oxide-semiconductor (CMOS) technology, hence low cost. A typical structure for an APD device is shown in Figure 3.1.



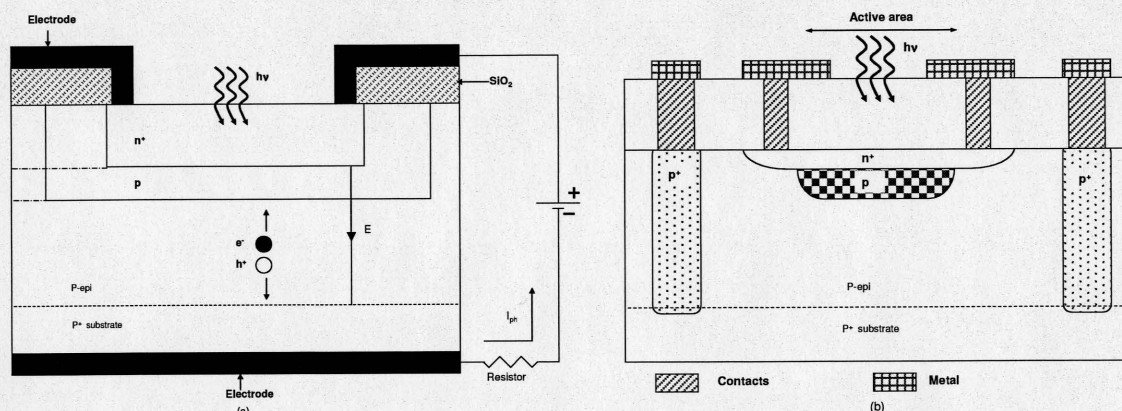


Figure 3.1 – Principle of detection of a typical APD is depicted in panel (a). Panel (b) illustrates a more complex design of an APD developed by C. Jackson for single photon detection (redrawn from S. Kasap and C. Jackson *et. al.* [50, 51]).

The n and p symbol refers to the type of chemical dopants added to the semiconductor where n refer to dopant with excess electron carrier and p to hole carrier. The principle of operation of an avalanche photodiode is described in panel (a) of figure 3.1. Briefly, a voltage is applied across the avalanche photodiode generating an electric field within the structure. Photons, with energy bigger than the band gap of the semiconductor, are absorbed within the active area of the avalanche photodiode generating an electron/hole pair. Because of the presence of high electric field, the electron is accelerated across the depletion region (area delimited by  $n^+$  and p shown in panel (a) of figure 3.1) and in doing so, exciting an adjacent carrier. The newly generated carrier will also be accelerated in the depletion region causing an excitation of another electron. An avalanche of carriers is observed within the APD generated through a multiplication phenomenon. The carriers are swept to the electrodes creating a measurable current, referred to as photocurrent. In-depth discussion on the principle of detection of complex



APD structures can be found elsewhere [49, 51, 52]. Our interest in this work is to use APDs as sensitive detection modalities.

Avalanche photodiodes operate in several modes; photodiode, avalanche photodiode, and Geiger mode. Depending on the biased voltage, APDs can operate as generic light detector or highly sensitive photodetector with single-photon detection capability. The latter modality, known as Geiger mode, is accomplished when the bias voltage across the APD is operated at a voltage larger than the breakdown voltage. An illustration showing the operational modes of APDs is presented in Figure 3.2. The applied voltage across the APD is shown on the x-axis while the measured current is depicted on the y-axis.

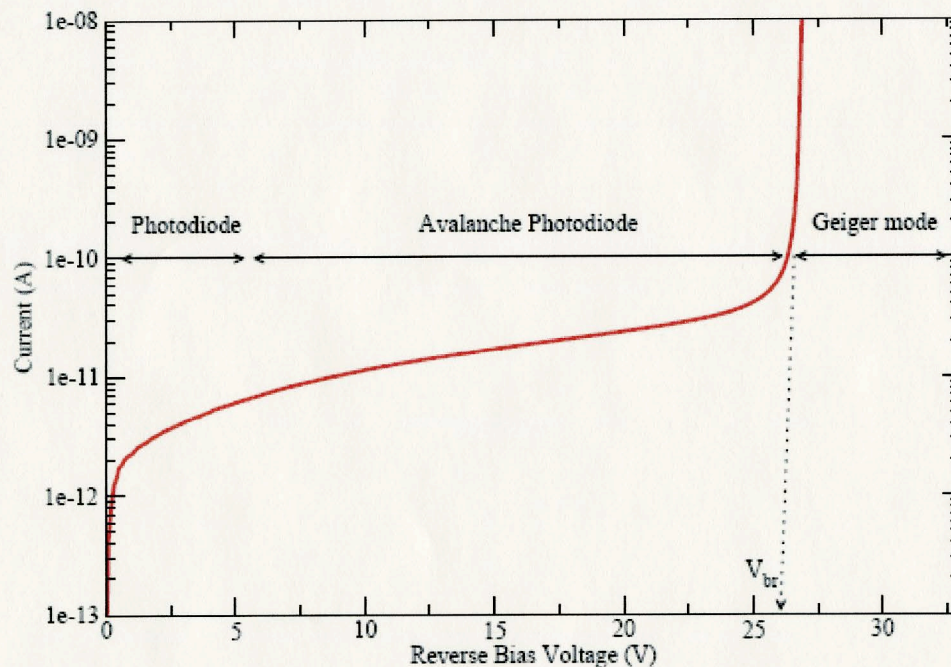


Figure 3.2 – Current vs. Voltage (IV) curve of an avalanche photodetector. The Geiger-mode is the region where APD can detect single photon. (Reprinted from C. Jackson with permission[49])

### 3.3 EXAMPLES OF APD APPLICATIONS

Avalanche photodiodes are widely used as photon detectors for light detection in optical communications. Their use is also prevalent in fluorimetry, especially for single molecule detection. For examples, APDs were used as detection modalities for fluorescence signal in DNA sequencing machine. In their effort to develop a capillary electrophoresis for DNA sequencing purposes, Zhang *et. al.* used APDs to detect fluorescence signals from solution within each capillary [53]. As a proof of concept, a laser source was used to excite fluorescein molecules within each capillary. The limit of detection of APDs was around 130 fluorescein molecules from an injected solution of  $2 \times 10^{-12}$  M. Crabtree *et. al.* also reported the high photon detection sensitivity of APDs in a similar study [54]. In addition, studies on single-molecule fluorescence detection employed APDs as detection systems. Gosch *et. al.* have demonstrated the use of APDs for single molecule detection in fluorescence correlation techniques as well as the determination of molecules concentrations [55]. Elsewhere, APDs were used to study conformational changes in p53 protein-related peptides [56]. Neuweiler *et. al.* employed APDs to detect the quenching of a fluorescent dye by tryptophan, which were conjugated to the peptide being studied. Others [57] have used APDs to determine fluorescence lifetimes measurements. The use of APDs for photon detection, specifically single photon, has been demonstrated indicating the powerful use of such systems for developing immunoassay-based biosensor.



### 3.4 CHARACTERIZATION OF PHOTODIODES

Avalanche Photodiodes were purchased from Carl Jackson (at the time Photondetection System Inc. now at SensL Inc., Ireland). Photodetectors as received were on bare die, arranged in 1-D arrays. Microelectronic packaging was implemented to provide a better handling of APDs instead of using micromanipulator. The packaging of APDs was done for each linear array of detectors. The packaging process commonly involves wire bonding of the device to the pins of the package in addition to epoxy resin coverage for electrical isolation. To provide a venue for surface functionalization, a coverslip was bonded to the epoxy with one side exposed to air. This process was performed at Advotech Inc (Tempe, AZ). A picture of the packaged device can be viewed in figure 3.3.

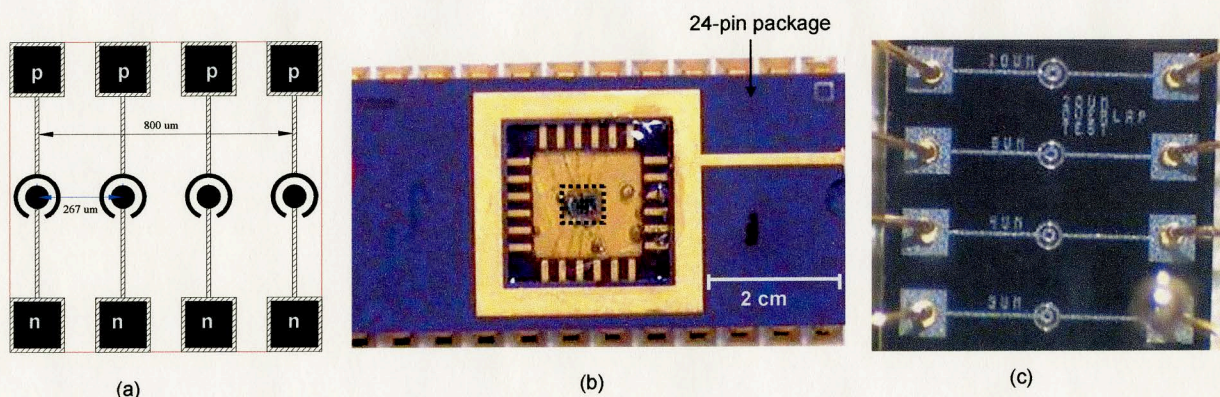


Figure 3.3 – As shown in the design layout of an APD array, the size of the array is slightly above  $1\text{mm}^2$ . Panel (b) shows a top-down view of a packaged APD. A magnified view of the dotted square is depicted in panel (c).

Prior to antibody immobilization onto the packaged device, I verified some of the characteristics of APDs. Namely, diode characteristics of the APDs, breakdown voltage and light detection were determined. The former two properties were done using a

current-voltage analyzer, which measures the current as the voltage is swept across the APD. A typical diode will have nonlinear current-voltage characteristics. One of our colleagues helped in the testing of APD (Electrical Engineering department, Arizona State University). Diode characteristics for one APD were observed as figure 3.4 indicates. In addition, the breakdown voltage for avalanche mode was between 26-27 V as shown in panel (b) of figure 3.4.

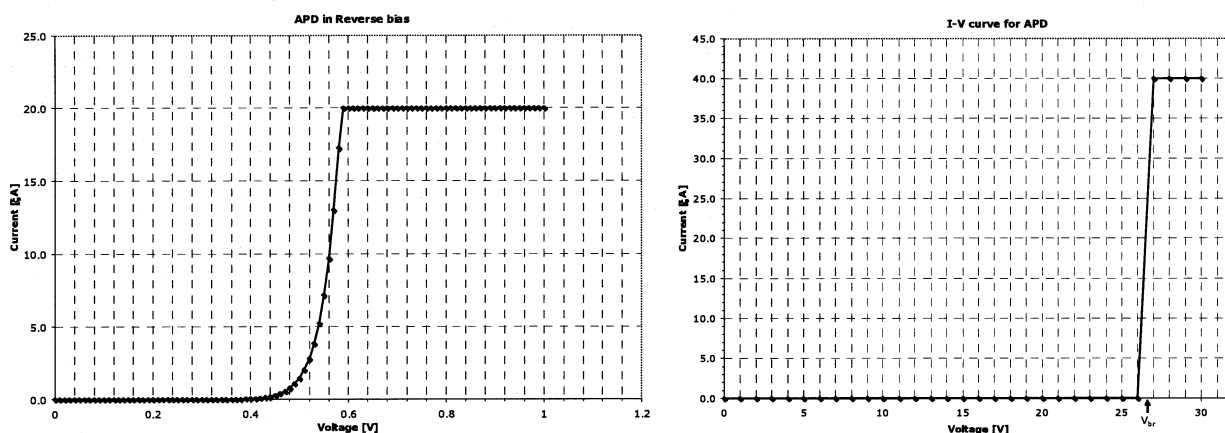


Figure 3.4 – Diode Characteristic (a) and Breakdown voltage (b).

Using light emitting diode (LED), a simple circuit was designed in order to test light detection characteristic of one APD. On a breadboard, a red LED in series with a resistor was placed right above the detector. The testing was done in a dark room to reduce stray light noise. The resistor used for the APDs was  $98.6 \text{ k}\Omega$  as measured using a voltmeter. The resistance value for the APD was chosen following results from C. Jackson [49]. The applied voltage across the APD was kept constant at 26.72V whereas the voltage across the red LED was varied from 0–4 V. Oscilloscope probes were placed across the



resistance in series with the APD to measure the response of APD. Figure 3.5 shows the setup used in this case.

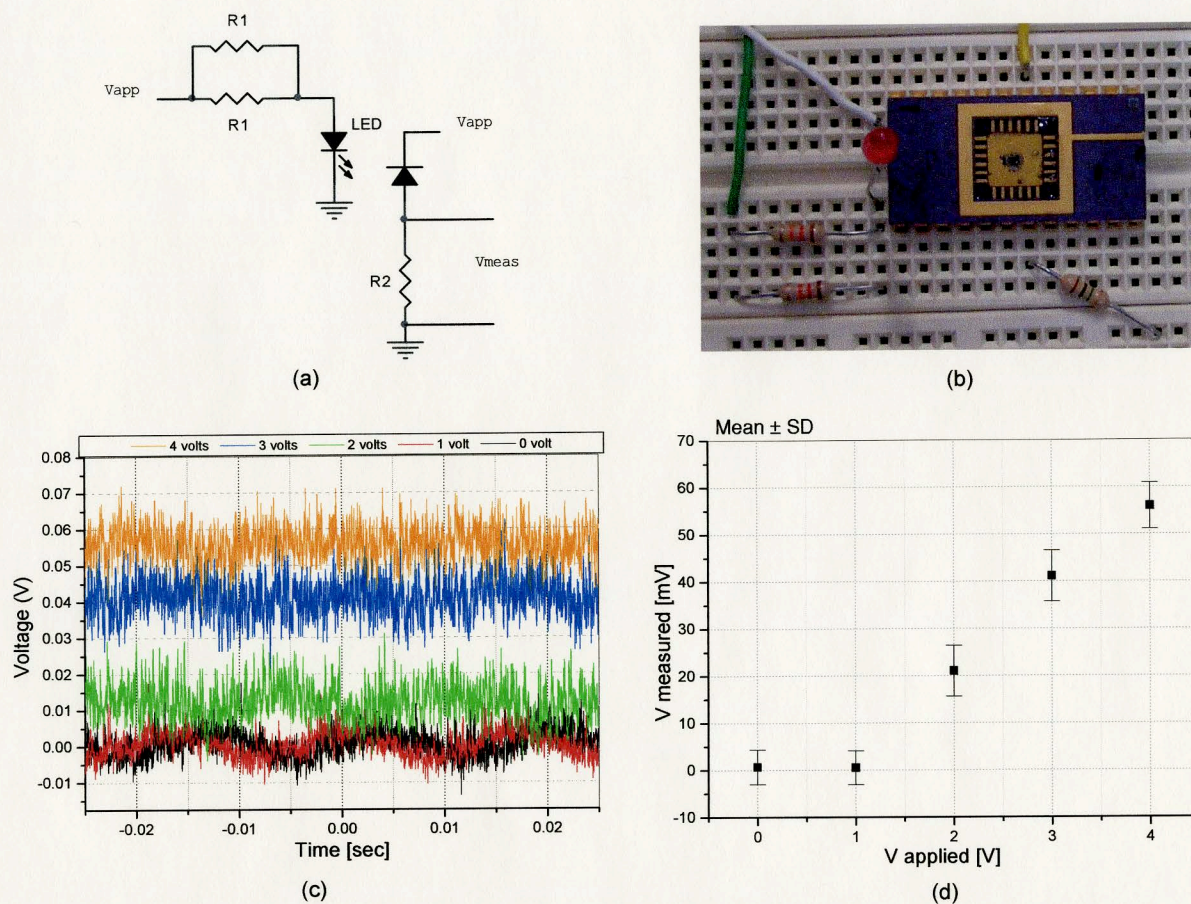


Figure 3.5 – APDs characterization using a red light emitting diode (LED). Shown in panels (a) and (b) are the circuits used to test the detection of light using APDs. The voltage across the red LED was varied from 0V to 4V changing the intensity of light. The voltage was measured across the resistor of the APD being tested using an oscilloscope. Panels (c) and (d) show the voltage readout indicating the capability of APDs to detect light emanating from the red LED.

As indicated in panel (d) of figure 3.5, the APD detected the response in light intensity as the voltage across the LED was varied. The next step is to integrate the APD with antibody discussed in the subsequent section.

### **3.5 APD DETECTION OF CHEMILUMINESCENCE**

Having determined that APDs are functioning as photodetectors, the immobilization of antibody onto the packages APD was performed. I have used the same immunoassays employed in chapter 2. Steps from the immunoassay procedure shown in figure 2.7 were adjusted in this case due to differences in the size of substrates and use of a package. The procedure for printing antibody on the coverslip of the APD is described in the following section.

#### **3.5.1 EXPERIMENTAL PROCEDURE**

Our objective is to demonstrate that APDs are able to detect the chemiluminescence signal from the immunoassay. Prior to antibody attachment, I verified that APDs detect light. The diameter of the APD's active area used, unless stated otherwise, for all subsequent measurements was 20  $\mu\text{m}$  biased at voltage of 26.72V. Prior each measurement, an oscilloscope was used to check the functional state of the APD. While a 26.72 V was applied across the APD, the voltage change was monitored on the oscilloscope as the room light was switched on. A change in voltage on the oscilloscope screen indicates that the APD is suitable for antibody attachment.

##### **i. GPTS coating of coverslip**

Within each APD package, a coverslip was bonded to the epoxy resin as previously described. The coverslip was rinsed with ethanol and blown dried with nitrogen. A stock solution of 2% (v/v) GPTS dissolved in hexane was used to coat the coverslip. For small-sized coverslip within the APD package, 300  $\mu\text{L}$  of the GPTS solution was. To prevent drying due to evaporation of hexane, I repeatedly added 300  $\mu\text{L}$  of 2% GPTS solution at

several time intervals for a total time of 2 hours. Thereafter, the coverslip was rinsed twice with hexane. It was then blown dry with N<sub>2</sub> stream and used immediately for antibody attachment.

### **ii. IgG attachment to APD**

As a proof of principle, one spot of a 1:500 (v/v) Mouse anti-human collagen type IV IgG (i.e. 1<sup>o</sup> Ab) solution dissolved in a PBS buffer was printed manually using a pipette. The volume of the 1<sup>o</sup> Ab droplet was 0.3 µl, which covered the whole APD array. Our goal is that 0.3 µl antibody solution be spotted on the coverslip directly above the 20µm APD (with 5µm guard ring). The immunoassay shown in figure 2.7 was followed with slight adjustment. For instance, the 1<sup>o</sup> Ab spot was left on the coverslip for 5 min before a rinsing step was performed. Should the 1<sup>o</sup> Ab solution be kept on the coverslip for longer time, the antibody will denature due to dehydration. A blocking solution of 2% (w/v) BSA in buffer was added to the APD package for 15 min. Another buffer rinse was performed and the APD package was placed in a 50 ml tube containing 1:10,000 Anti-mouse IgG conjugated to HRP. The incubation of APD package in the 2<sup>o</sup> Ab solution was for 40 min with agitation on a rocking plate during the last 20 min of incubation. The APD packaged was then rinsed with PBS buffer and placed in a 50 ml tube containing a 10 ml solution of a chemiluminescent substrate.

### **iii. APD detection of chemiluminescence.**

In a dark room, probes of the power supply set to 26.72 V and oscilloscope were connected to their corresponding wires placed in the breadboard. Depending on availability, I have used a Tektronix TDS 1012 (20 MHz) or an Agilent (MSO6104A,



1GHz) oscilloscope. After the incubation in chemiluminescence, the antibody-coated APD was withdrawn with the package pins dried prior insertion into the breadboard. A black box was used to prevent stray light (power supply and oscilloscope screens) from interfering with measurements. Immediately, the power supply was turned on and the voltage measurements displayed on the oscilloscope were saved on a flash drive. Data acquisition of voltage was done for different time intervals reaching 1 hr. A typical oscilloscope displays at two different time sets are shown in figure 3.6.

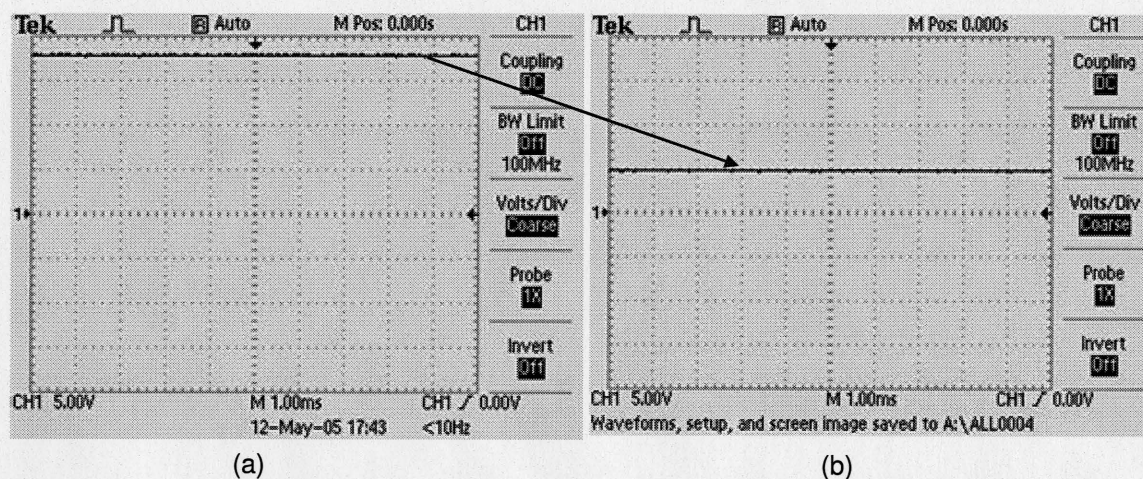


Figure 3.6 – Oscilloscope output. Voltage is labeled as y-axis (note 5V per division). Voltage values shown in panels (a) and (b) are taken at two different time intervals. The decrease in voltage is due to the decay of chemiluminescence over time.

As a control experiment, a 0.3  $\mu\text{l}$  spot of PBS buffer solution was printed on a GPTS coated coverslip of another APD package. To be consistent with our experiments, I only used 20  $\mu\text{m}$  active area with 5  $\mu\text{m}$  guard ring of the new APD. The immunoassay was repeated as described previously and data acquisition was done according to the previous procedure. The ‘control’ is done to prove that the chemiluminescence observed is due to

1°Ab-2°Ab interactions. However, 2°Ab present in the bulk solution add noise to our measurements.

The attachment of Mouse anti-human type IV collagen was repeated for additional two trials. For each experiment, a control measurement was performed in parallel. Because of a limited number of available APD packages (2 packages), cleaning of used APD packages was performed. To make sure that past GPTS coating is removed, I used a 1:5 piranha solution. The coverslip for each APD package was cleaned by adding a droplet of the piranha solution. Careful consideration during piranha cleaning was taken to avoid etching the surrounding area of the package. The coverslip was scrubbed hastily with a cotton swab, rinsed thoroughly in water, and dried under a stream of nitrogen. The newly cleaned APD packages are ready for another round of GPTS coating.

### **3.5.2 RESULTS AND DISCUSSION**

Following the first two immunoassay experiments, APD packages were cleaned as previously described in order to perform additional experiments. Prior to GPTS coating, each APD package was tested for light detection in a dark room simply by switching the light. A voltage change as the light was switched on/ off indicated the usability of the device. This 'crude' method was performed after further piranha cleaning. The performance of the APD did not vary dramatically after each cleaning step as figure 3.7 shows.

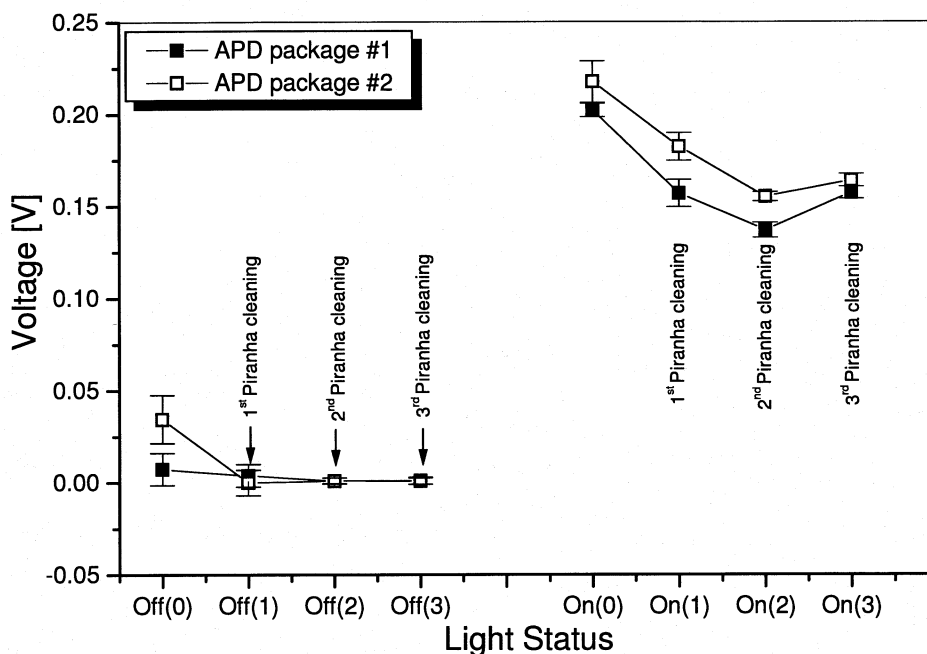


Figure 3.7 – Reusability of APD packages after a piranha cleaning procedure. The number in parentheses on the x-axis indicates the number of piranha cleaning performed. The cleaning allowed us to use the two APD packages to perform eight experiments.

Although cleaning APD packages proved useful, I cannot ascertain whether the piranha solution etched away the GPTS coating on the coverslip. I presume that this is highly likely due to the acidic nature of piranha solution. However, in designing a commercial immunoassay based microdevice, a less corrosive solution would be preferable to clean the devices to avoid damage to the APD package and waste management control.

The attachment of mouse anti-human collagen type IV IgG was verified using an immunoassay with a labeled secondary antibody, namely anti-mouse IgG conjugated to HRP. APDs were able to detect the chemiluminescence light as observed in figure 3.8.



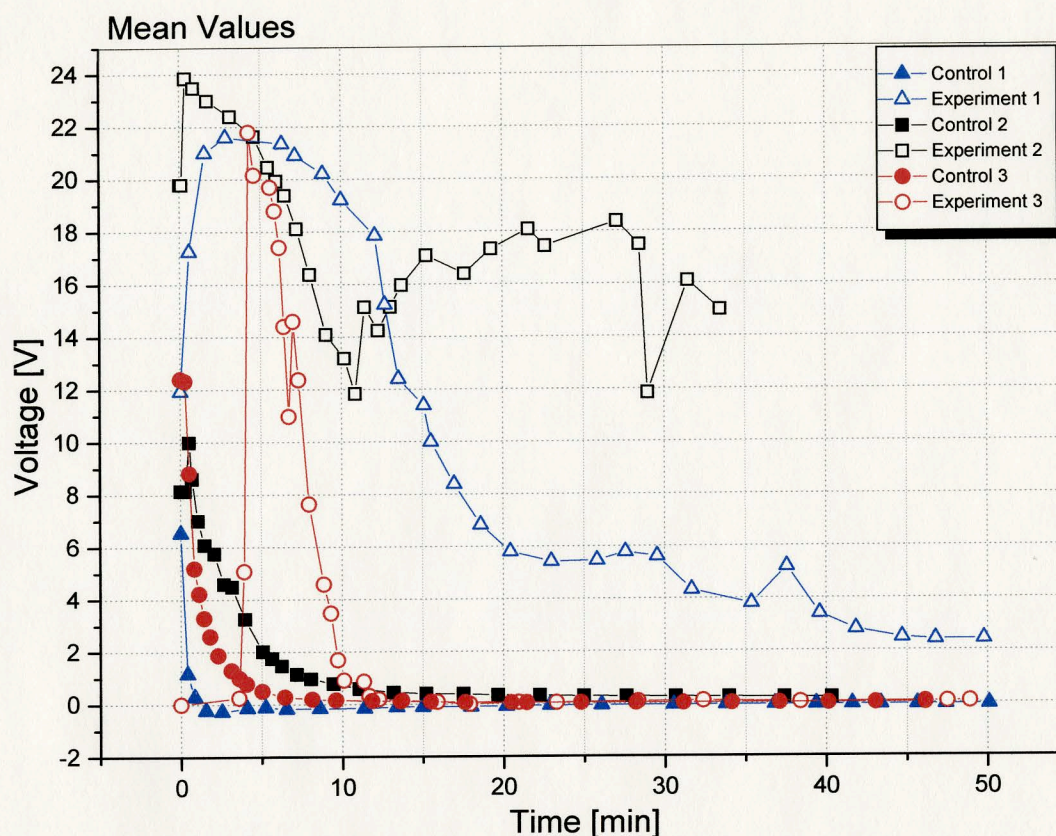


Figure 3.8 – APD detection of chemiluminescence. ‘Experiment’ refers to  $1^{\circ}$  Ab attached to APD whereas ‘control’ refers to PBS being printed on APDs. Clearly, APDs are sensing the secondary Ab recognition of the primary Ab as indicated by the difference in voltages between ‘experiments’ ( $\Delta$ ,  $\square$ , and  $\circ$ ) and ‘controls’ ( $\blacktriangle$ ,  $\blacksquare$ , and  $\bullet$ ).

Figure 3.8 contains data from six different measurements including experiment and control. As expected, the variation of the chemiluminescent intensity is observed with the control experiment showing a decreasing voltage over time. The intensity from this is due to the bulk presence of secondary antibody that reacted with the chemiluminescent substrate. On the other hand, the presence of  $1^{\circ}$  Ab results in a typical chemiluminescent variation over time (e.g. open triangles in figure 3.8). One striking feature is the large variance observed for APD packages immobilized with  $1^{\circ}$ Ab (open symbols). The

position of the antibody spot printed on the coverslip will affect the signal intensity (in this case, the value of the voltage measured). A second speculation would relate to whether the difference between the amount of 1°Ab manually spotted is significant. One way to avoid such error is to use a mechanical printer, which deposits droplets with low variance in spot volume. On the upside, results shown in figure 3.4 indicate for one thing that APDs are able to detect chemiluminescence. Furthermore, there are clear differences between control values (noise signal) and true experimental values. Background subtraction should have been done in this case, however the discrepancies in the time intervals between control and experiment would not provide useful information.

In addition, I have used APDs in conjunction with the immunoassay based on Mouse monoclonal anti-biotin IgG and HRP-tagged biotin. This assay will validate that the antibody retains its activity of the surface and the active site of the antibody is exposed to the analyte solution. The procedure for attaching Mouse anti-biotin IgG is identical to attachment of mouse anti-human collagen type IV. One difference is the dilution factor used which was 1:100 mouse anti-biotin IgG in PBS solution. The biotin-HRP solution was prepared from a 0.75 mg/ml with a dilution factor of 1:2000. For the control experiment, a buffer solution was added instead of the biotin conjugated to HRP to the sensors. Results from such experiments are depicted in figure 3.9.



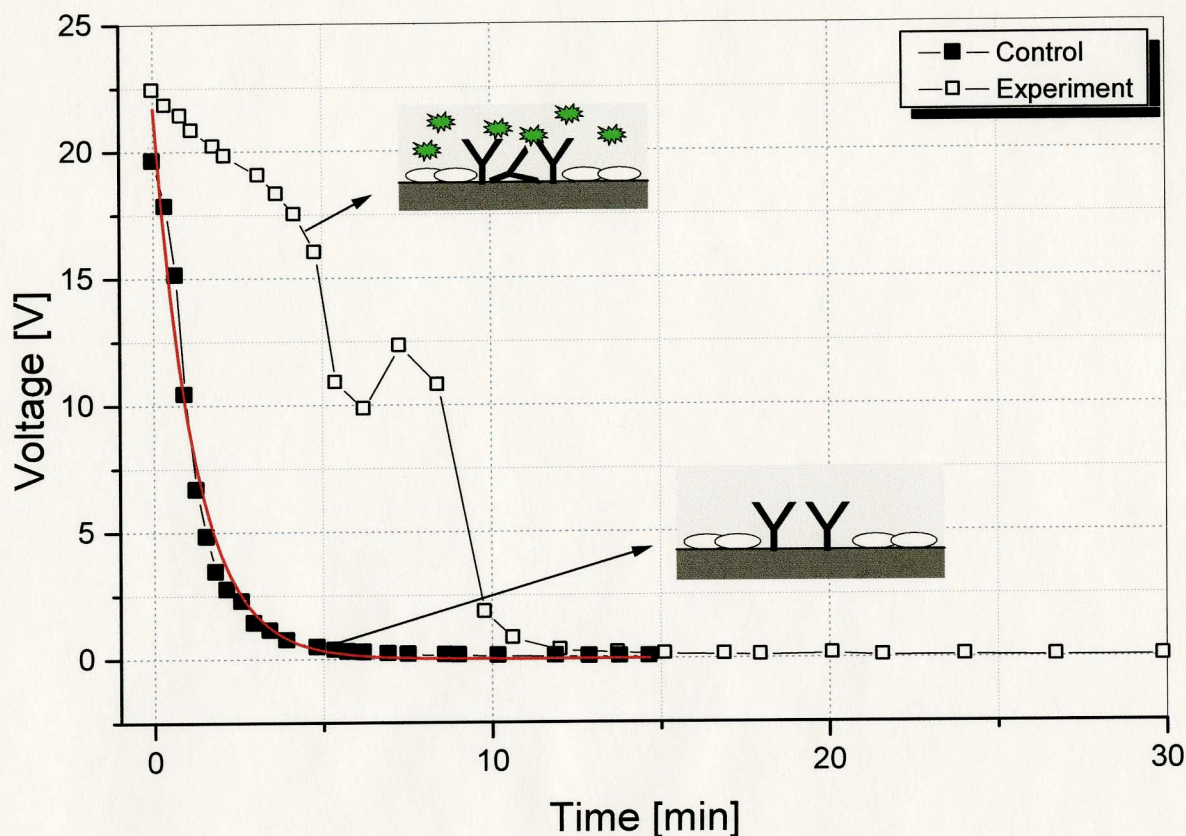


Figure 3.9 – APD detection of chemiluminescence using an immunoassay based on anti-biotin IgG-biotin conjugated to HRP interactions. Experimental schemes used are shown.

It is expected *a priori* that a control measurement using the immunoassay, i.e. no analytes added, should have voltage values fluctuated around zero as no HRP was used. However, figure 3.9 shows a different scenario for control measurements manifested by a rapid decay of the voltage values. In an effort to explain the voltage decay from control measurement, chemiluminescent substrates used for HRP were mixed together without adding protein conjugated to HRP. In the dark room, a visible yet dim chemiluminescent light was observed. It may be that the presence of oxygen in the atmosphere is reacting with the chemiluminescent substrates. In fact, chemiluminescence is often the result of a



reaction between a chemiluminescent substrate and oxygen. What is interesting about the voltage values for the control experiment is that an exponential decay curve can be fitted (red line in figure 3.9). This will help us perform a background subtraction as time values for 'control' and 'experiment' shown on the x-axis of figure 3.9 do not coincide.

An exponential decay function was fitted to the voltage values for 'control' measurements. The fitted equation has the form:

$$V = 21.696 \cdot e^{-t/1.19279} \quad \text{Equation 3-1}$$

Where  $V$  represents voltage and  $t$  represents time in min.

Using equation 3.1, time values from the experiment using biotin conjugated to HRP were inserted. The voltage values obtained using equation 3-1 are estimated values for the 'control' experiment. In doing so, I can perform background subtraction because signals are now "measured" at similar time intervals. A background subtraction was performed, i.e. voltage values estimated using the method just mentioned for 'control' were subtracted from voltage values for experiment based on biotin conjugated to HRP. The result of background subtraction is summarized in figure 3.10.

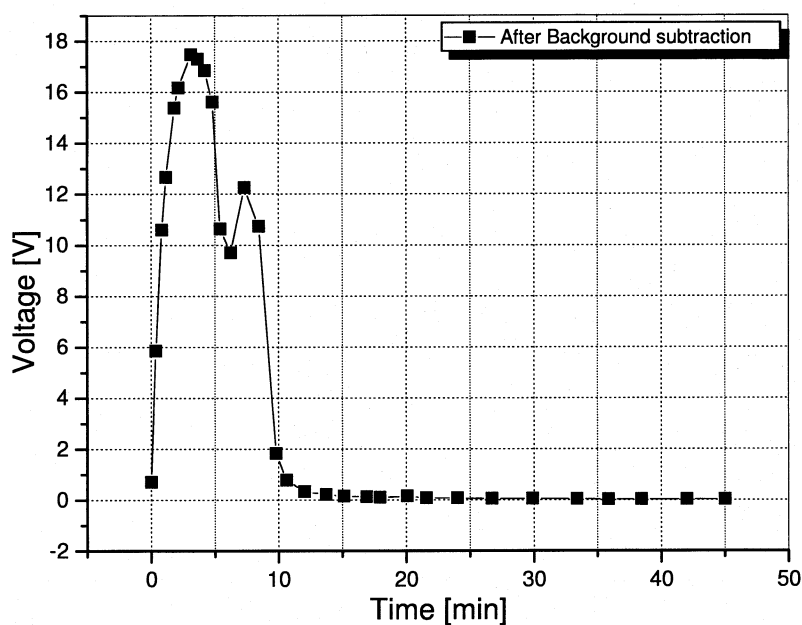


Figure 3.10 – APD detection of chemiluminescence after background subtraction. The curve is more descriptive of the chemiluminescence decay in the presence of HRP.

### 3.6 SUMMARY AND CONCLUSION

In this chapter, antibodies were immobilized on APDs using a silane-based coating characterized in chapter 2. APDs detection of chemiluminescence was observed. In addition, APDs were able to detect difference in voltage values between control and experiment measurements. The antibody-based biosensor combined the specificity of immunoassay with the sensitivity of avalanche photodiodes. In addition, the current device setup provides portability and can be manufactured at a low cost. However, device optimization will be required in order to elucidate the potential use of such device. I believe the on-chip readout and the miniaturization of the device are appealing features for developing commercial biosensors

## **CHAPTER 4**

### **SUMMARY AND FUTURE WORK**

#### **4.1 SUMMARY**

Immunoassay technologies are widely used for biomolecules identification in clinical diagnostics, screening food pathogen, and biomolecular research. Immunoassay techniques offer high specificity and sensitivity for molecular screening applications. When labeled analytes are used, an optical detection technique is often required. Most detection techniques have been based on fluorescence microscopy, autoradiography, or CCD imaging for chemiluminescence detection. Such techniques are not suited for fieldwork and at point of care situations. In addition, these techniques are expensive. Hence, the need for low cost, mobile commercial biosensors is desirable. In this work, I have presented an example of an immunoassay-based sensor with design specifications aforementioned. Our biosensor is based on the integration of immunoassay technology with an avalanche photodiode, a highly sensitive photondetection system.

I have shown qualitatively that antibodies attached to the modified oxide layer of silicon substrates retained their bioactivity to recognize its specific analyte. This was demonstrated using an immunoassay whose components were mouse monoclonal anti-biotin IgG and biotin molecules conjugated to HRP. In addition, APDs coupled to antibodies detected the chemiluminescence light from the previous immunoassay. There were clear differences between signals from control experiments and actual experiments. The small size of APD packages used for microsensing offers mobility, portability, fast

readout, and low cost. Further analysis of the immunoassay-based microdevice is needed to verify its use in screening multiple target, providing a user-friendly readout, and packaging.

## 4.2 FUTURE WORK

As a proof of concept, I have shown that APDs integrated with antibody are able to detect chemiluminescence light. Light detection data were displayed in graphical representation as shown in figures 3.8–3.10. Digital readout of chemiluminescence indicating the presence of analytes in solution is more preferred than the current graphical layout of data for a commercial readout. In addition, the readout system must perform background subtraction and output data indicating with statistical significance the presence of targeted molecules in solution. Prior to the development of a digital readout system, I need to address the following issues:

1. The limit of detection of APDs should be determined. As mentioned in chapter 3 APDs when operated in Geiger mode can detect single photon. In theory, picomolar and even femtomolar protein concentration should be detected. I had limited number of APD packages, and hence I was unable to perform such tests as such demand more than two APD packages.
2. Use APDs in human sera to screen for a targeted disease-causing protein. As a proof of concept, I can follow in the footsteps of Askari *et. al.* [40] in designing antibody-based biochip for cancer diagnostics. Serum samples from healthy patients could be isolated and mixed with a series of anti-p53 antibody concentration. Thereafter, APDs



attached to p53 proteins will be used to detect the presence of anti-p53 antibody. I need to mention that conjugation of anti-p53 antibody to HRP should be performed.

3. Another projected study should focus on using a microarray printer to spot protein solution onto APDs array. Each protein spot should be printed on top of each APD within a linear array of APDs. This step requires APDs with active area larger Another aspect that should be addressed is the need for larger active area than 20 $\mu$ m (used in this project However, APDs with larger active area are commercially available. The question then is demonstrating the integration of microarray technology with CMOS-based APDs. In addition, demonstrating high throughput screening using the currently developed immunoassay microdevice will be a step closer to commercialization. Indeed, microarray technology potential for high density printing of protein have been demonstrated [9, 26, 36, 38]. Microarray technology combined with CMOS-based APD technology will be useful in developing a commercial high throughput device for biosensing application.
4. Last, but not least, research effort should focus on improving the optics of the immunoassay-based microdevice related to including antireflection coating to reduce photon loss due to reflection. In addition, a system of lenses is desired for each antibody microarray that will focus chemiluminescence from each protein spot onto APDs. Micro-optics technology could be used to design a microlens array, which will be incorporated on the coverslip of APD package. The microlens system will improve the optical characteristic of the immunoassay-based microdevice. In fact, Silica-based microlens, which can be functionalized and immobilized with antibodies, are

available commercially. A virtual setup of the device for 1x4 APD array with a microlens array is illustrated in figure 4.1.

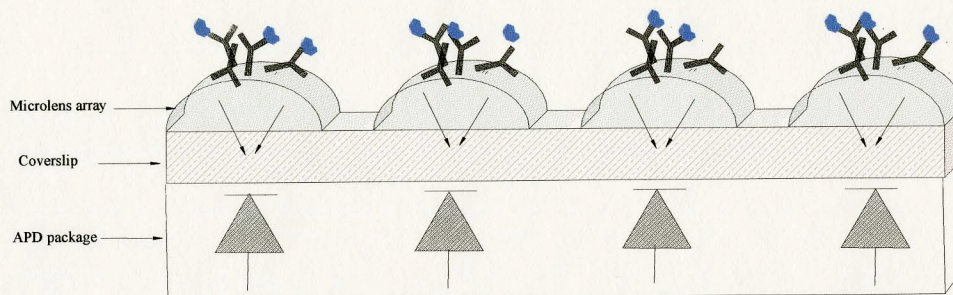


Figure 4.1 - Improving the optics of the developed immunoassay-based microdevice.

Using a microlens system, light from immunoassay can be focused onto APDs as shown in figure 4.1. The coverslip in the layout shown in figure 4.1 provides a smooth surface for fabricating the microlens system.

## APPENDIX A

## PERMISSIONS



LeeHouse  
Bessboro Road  
Blackrock, Cork, Ireland  
Tel: +35321 4350442  
Fax: +35321 4350447  
Email: [info@SensL.com](mailto:info@SensL.com)  
Web: [www.SensL.com](http://www.SensL.com)

Re: Permission to reproduce Figure 3.11 from J. C. Jackson's Ph.D. Thesis

As per request by Maurice Jabbour, I hereby grant permission to reproduce Figure 3.11 from page 55 of my thesis as published. Full reference to the thesis is listed below for acknowledgement purposes.

J. Carlton Jackson  
*Geiger-Mode Avalanche Photodiodes*  
Ph.D. Thesis  
Submission Date: April 2003  
University College Cork  
Cork, Ireland

Please contact me if any additional information is required.

Regards,

A handwritten signature in black ink, appearing to read 'J. Carlton Jackson'.

J. Carlton Jackson  
CTO

SensL Technologies Limited: Registered in Ireland, Registration No. 384217  
Directors: D. Berkery, J. Gantly, J. C. Jackson, J. O'Keeffe

## REFERENCES

1. D'Orazio, P., *Biosensors in clinical chemistry*. Clin Chim Acta, 2003. **334**(1-2): p. 41-69.
2. Lippa, P.B., L.J. Sokoll, and D.W. Chan, *Immunosensors--principles and applications to clinical chemistry*. Clin Chim Acta, 2001. **314**(1-2): p. 1-26.
3. Byfield, M.P. and R.A. Abuknesha, *Biochemical Aspects of Biosensors*. Biosensors & Bioelectronics, 1994. **9**(4-5): p. 373-400.
4. Keusgen, M., *Biosensors: new approaches in drug discovery*. Naturwissenschaften, 2002. **89**(10): p. 433-444.
5. Templin, M.F., et al., *Protein microarray technology*. Drug Discovery Today, 2002. **7**(15): p. 815-822.
6. Jain, K.K., *Current status of molecular biosensors*. Med Device Technol, 2003. **14**(4): p. 10-5.
7. Schwenk, J.M., et al., *Cell microarrays: an emerging technology for the characterization of antibodies*. Biotechniques, 2002. **Suppl**: p. 54-61.
8. Kohler, G. and C. Milstein, *Continuous cultures of fused cells secreting antibody of predefined specificity*. Nature, 1975. **256**(5517): p. 495-7.
9. Xu, Q. and K.S. Lam, *Protein and Chemical Microarrays-Powerful Tools for Proteomics*. J Biomed Biotechnol, 2003. **2003**(5): p. 257-266.
10. Wahlgren, M. and T. Arnebrant, *Protein adsorption to solid surfaces*. Trends Biotechnol, 1991. **9**(6): p. 201-8.
11. Chen, S.F., et al., *Controlling antibody orientation on charged self-assembled monolayers*. Langmuir, 2003. **19**(7): p. 2859-2864.
12. Li, L.Y., S.F. Chen, and S.Y. Jiang, *Protein adsorption on alkanethiolate self-assembled monolayers: Nanoscale surface structural and chemical effects*. Langmuir, 2003. **19**(7): p. 2974-2982.
13. Zhang, F. and M. Srinivasan, *Self-assembled Molecular Films of Aminosilanes and Their Immobilization capacities*. Langmuir, 2004. **20**: p. 2309-2314.
14. Veiseh, M., M.H. Zareie, and M.Q. Zhang, *Highly selective protein patterning on gold-silicon substrates for biosensor applications*. Langmuir, 2002. **18**(17): p. 6671-6678.



15. Zhu, H., et al., *Global analysis of protein activities using proteome chips*. Science, 2001. **293**(5537): p. 2101-5.
16. Wong, S., *Chemistry of Protein Conjugation and Cross-linking*. 1991, Boca Raton: CRC Publisher.
17. Vanderberg, E.T., et al., *Structure of 3-Aminopropyl Triethoxy Silane on Silicon Oxide*. Journal of Colloid and Interface Science, 1991. **147**(1): p. 103-118.
18. Akkoyun, A. and U. Bilitewski, *Optimisation of glass surfaces for optical immunosensors*. Biosens Bioelectron, 2002. **17**(8): p. 655-64.
19. Hu, M.H., et al., *Structure and morphology of self-assembled 3-mercaptopropyltrimethoxysilane layers on silicon oxide*. Applied Surface Science, 2001. **181**(3-4): p. 307-316.
20. Wang, H., et al., *Probing the Orientation of Surface-Immobilized Immunoglobulin G by Time-of-Flight Secondary Ion Mass Spectrometry*. Langmuir, 2004. **20**: p. 1877-1887.
21. Shin, D.S., et al., *Protein patterning by maskless photolithography on hydrophilic polymer-grafted surface*. Biosensors & Bioelectronics, 2003. **19**: p. 485-494.
22. Metzger, S.W., et al., *Development and characterization of surface chemistries for microfabricated biosensors*. Journal of Vacuum Science & Technology A, 1999. **17**(5): p. 2623-2628.
23. Taitt, C.R., et al., *Detection of Salmonella enterica serovar typhimurium by using a rapid, array-based immunosensor*. Appl Environ Microbiol, 2004. **70**(1): p. 152-8.
24. Orth, R.N., T.G. Clark, and H.G. Craighead, *Avidin-Biotin micropatterning methods for biosensors applications*. Biomedical microdevices, 2003. **5**(1): p. 29-34.
25. Yu, H. and J.G. Bruno, *Immunomagnetic-electrochemiluminescent detection of Escherichia coli O157 and Salmonella typhimurium in foods and environmental water samples*. Appl Environ Microbiol, 1996. **62**(2): p. 587-92.
26. Delehanty, J.B. and F.S. Ligler, *Method for printing functional protein microarrays*. Biotechniques, 2003. **34**(2): p. 380-385.
27. Predki, P.F., *Functional protein microarrays: ripe for discovery*. Current Opinion in Chemical Biology, 2004. **8**: p. 8-13.
28. Midwood, K.S., et al., *Easy and Efficient Bonding of Biomolecules to an Oxide Surface of Silicon*. Langmuir, 2004. **20**: p. 5501-5505.

29. Ostuni, E., et al., *A survey of structure-property relationships of surfaces that resist the adsorption of protein*. Langmuir, 2001. **17**(18): p. 5605-5620.
30. Lee, C.S., et al., *Protein patterning on silicon-based surface using background hydrophobic thin film*. Biosensors & Bioelectronics, 2003. **18**(4): p. 437-444.
31. Sweryda-Krawiec, B., et al., *A New Interpretation of Serum Albumin Surface Passivation*. Langmuir, 2004. **20**: p. 2054-2056.
32. Delamarche, E., et al., *Patterned delivery of immunoglobulins to surfaces using microfluidic networks*. Science, 1997. **276**(5313): p. 779-781.
33. Blawas, A.S. and W.M. Reichert, *Protein patterning*. Biomaterials, 1998. **19**(7-9): p. 595-609.
34. Renault, J.P., et al., *Fabricating Arrays of Single Protein Molecules on Glass Using Microcontact Printing*. J. Phys. Chem. B, 2002. **107**(3): p. 703-711.
35. Morozov, V.N. and T.Y. Morozova, *Electrospray deposition as a method for mass fabrication of mono- and multicomponent microarrays of biological and biologically active substances*. Analytical Chemistry, 1999. **71**(15): p. 3110-3117.
36. Michaud, G.A., et al., *Analyzing antibody specificity with whole proteome microarrays*. Nat Biotechnol, 2003. **21**(12): p. 1509-12.
37. MacBeath, G. and S.L. Schreiber, *Printing proteins as microarrays for high-throughput function determination*. Science, 2000. **289**(5485): p. 1760-1763.
38. Haab, B.B., M.J. Dunham, and P.O. Brown, *Protein microarrays for highly parallel detection and quantitation of specific proteins and antibodies in complex solutions*. Genome Biol, 2001. **2**(2): p. RESEARCH0004.
39. Moreno-Bondi, M.C., J.P. Alarie, and T. Vo-Dinh, *Multi-analyte analysis system using an antibody-based biochip*. Anal Bioanal Chem, 2003. **375**(1): p. 120-4.
40. Askari, M., et al., *Application of an antibody biochip for p53 detection and cancer diagnosis*. Biotechnol Prog, 2001. **17**(3): p. 543-52.
41. Baird, C.L. and D.G. Myszka, *Current and emerging commercial optical biosensors*. J Mol Recognit, 2001. **14**(5): p. 261-8.
42. Rich, R.L. and D.G. Myszka, *Survey of the year 2003 commercial optical biosensor literature*. J Mol Recognit, 2005. **18**(1): p. 1-39.
43. Homola, J., *Present and future of surface plasmon resonance biosensors*. Anal Bioanal Chem, 2003. **377**(3): p. 528-39.

44. Johnsen, B.B., K. Olafsen, and A. Stori, *Reflection-absorption FT-IR studies of the specific interaction of amines and an epoxy adhesive with GPS treated aluminium surfaces*. International Journal of Adhesion and Adhesives, 2003. **23**(2): p. 157-165.
45. McGovern, M.E., K.M. Kallury, and M. Thompson, *Role of Solvent on the Silanization of Glass with Octadecyltrichlorosilane*. Langmuir, 1994. **10**(10): p. 3607-3614.
46. Campbell, A.K., *Chemiluminescence*. Ellis Horwood Series in Biomedicine. 1988, Chichester: VCH.
47. Kim, B.B., V.V. Pisarev, and A.M. Egorov, *A Comparative Study of Peroxidases from Horse Radish and Arthromyces ramosus as Labels in Luminol-Mediated Chemiluminescent Assays*. Analytical Biochemistry, 1991. **199**: p. 1-6.
48. Easton, P.M., et al., *Quantitative Model of the Enhancement of Peroxidase-Induced Luminol Luminescence*. J. Am. Chem. Soc., 1996. **118**: p. 6619-6624.
49. Jackson, J.C., *Geiger-Mode Avalanche Photodiodes*, in *National Microelectronics Research Centr.* 2003, National University of Ireland: Cork. p. 194.
50. Jackson, J.C., et al. *Process monitoring and defect characterization of single photon avalanche diodes*. in *Proceedings IEEE International Conference on Microelectronic Test Structures*. 2001.
51. Kasap, S.O., *Photodetectors*, in *Optoelectronics and Photonics: Principles and Practices*. 2001, Prentice Hall: Upper Saddle River, NJ. p. 217-250.
52. Agrawal, G.P., *Photodetectors*, in *Lightwave Technology: Components and Devices*. 2004, Wiley-Interscience: Hoboken, NJ. p. 253-286.
53. Zhang, J., et al., *A multiple-capillary electrophoresis system for small-scale DNA sequencing and analysis*. Nucleic Acids Res, 1999. **27**(24): p. e36.
54. Crabtree, H.J., et al., *Construction and evaluation of a capillary array DNA sequencer based on a micromachined sheath-flow cuvette*. Electrophoresis, 2000. **21**(7): p. 1329-35.
55. Gosch, M., et al., *Parallel single molecule detection with a fully integrated single-photon 2x2 CMOS detector array*. J Biomed Opt, 2004. **9**(5): p. 913-21.
56. Neuweiler, H., et al., *Measurement of submicrosecond intramolecular contact formation in peptides at the single-molecule level*. J Am Chem Soc, 2003. **125**(18): p. 5324-30.

57. Trabesinger, W., et al., *Continuous real-time measurement of fluorescence lifetimes*. Review of Scientific Instruments, 2002. **73**(8): p. 3122-3124.